Review on airflow in unsaturated zones induced by natural forcings

Xingxing Kuang,[1] Jiu Jimmy Jiao,[1] and Hailong Li[2]

Received 14 March 2013; revised 20 June 2013; accepted 12 July 2013; published 9 October 2013.

[1] Subsurface airflow in unsaturated zones induced by natural forcings is of importance in many environmental and engineering fields, such as environmental remediation, water infiltration and groundwater recharge, coastal soil aeration, mine and tunnel ventilation, and gas exchange between soil and atmosphere. This review synthesizes the published literature on subsurface airflow driven by natural forcings such as atmospheric pressure fluctuations, topographic effect, water table fluctuations, and water infiltration. The present state of knowledge concerning the mechanisms, analytical and numerical models, and environmental and engineering applications related to the naturally occurring airflow is discussed. Airflow induced by atmospheric pressure fluctuations is studied the most because of the applications to environmental remediation and transport of trace gases from soil to atmosphere, which are very important in understanding biogeochemical cycling and global change. Airflow induced by infiltration is also an extensively investigated topic because of its implications in rainfall infiltration and groundwater recharge. Airflow induced by water table fluctuations is important in coastal areas because it plays an important role in coastal environmental remediation and ecological systems. Airflow induced by topographic effect is studied the least. However, it has important applications in unsaturated zone gas transport and natural ventilation of mines and tunnels. Finally, the similarities and differences in the characteristics of the air pressure and airflow are compared and future research efforts are recommended.

Citation: Kuang, X., J. J. Jiao, and H. Li (2013), Review on airflow in unsaturated zones induced by natural forcings, *Water Resour. Res.*, *49*, 6137–6165, doi:10.1002/wrcr.20416.

1. Introduction

[2] Airflow in subsurface porous medium can be induced by various natural forcings, such as atmospheric pressure fluctuations, topographic effect, water table fluctuations, and infiltration. The induced airflow has important implications for a number of environmental, engineering, ecological, and hydrological problems. Subsurface airflow induced by atmospheric pressure fluctuations may play an important role in the environmental remediation of soil contaminated by volatile organic compounds (VOCs) in the unsaturated zone [e.g., *Auer et al*., 1996; *Tillman et al*., 2001]. Advective flows within soils induced by atmospheric pressure fluctuations can significantly influence the exchange rate of many trace gases (e.g., CO_2, CH_4, N_2O, and water vapor) from the subsurface to the atmosphere [e.g., *Baldocchi and Meyers*, 1991; *Massman et al*., 1997; *Christophersen et al*., 2001; *Massman*, 2006]. These trace gases are important to understand biogeochemical cycling, global change, and global gas balance [e.g., *Mattson and Likens*, 1990; *Massman et al*., 1997; *Turcu et al*., 2005; *Luo and Zhou*, 2006; *Massman*, 2006; *Weisbrod et al*., 2009; *Nachshon et al*., 2012]. The fluctuations of atmospheric pressure also affect the flow of radon from soil to the atmosphere [e.g., *Clements and Wilkening*, 1974; *Schery and Gaeddert*, 1982; *Schumann et al*., 1992]. *Schulz et al*. [2009] presented observations and numerical modeling results to show that atmospheric tides can trigger movement in an ongoing landslide. Furthermore, airflow induced by infiltration has two important implications: rainfall infiltration and groundwater recharge.

[3] The purpose of this paper is to present the state of knowledge on subsurface airflow induced by the natural forcings and to discuss the applications of the induced airflow. Governing equations will be presented and corresponding analytical and numerical models will be summarized. Field and laboratory experimental results will also be presented to clarify the phenomena and to demonstrate the effects of the induced airflow.

2. Airflow Induced by Atmospheric Pressure Fluctuations

2.1. Fluctuations of Atmospheric Pressure

[4] The standard atmospheric pressure (barometric pressure) is 101.325 kPa. Atmospheric pressure on the Earth's surface changes with time. The fluctuations of surface atmospheric pressure are caused by several reasons: (1)

[1]Department of Earth Sciences, University of Hong Kong, Hong Kong, China.
[2]State Key Laboratory of Biogeology and Environmental Geology and School of Water Resources and Environmental Science, China University of Geosciences, Beijing, China.

Corresponding author: J. J. Jiao, Department of Earth Sciences, University of Hong Kong, Pokfulam Road, Hong Kong, China. (jjiao@hku.hk)

0043-1397/13/10.1002/wrcr.20416

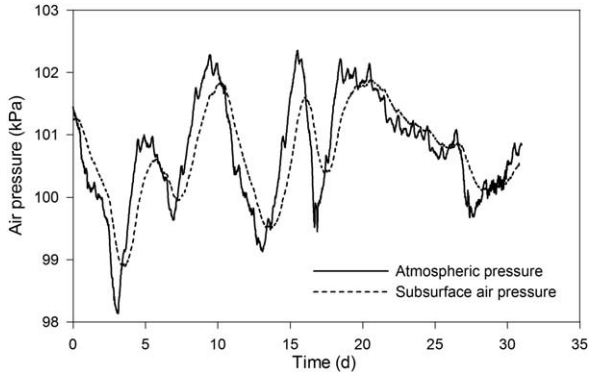

Figure 1. Atmospheric and subsurface air pressure measurements at a piezometer MHV 3A (modified from *Rossabi and Falta* [2002]). The subsurface air pressure was measured at a depth 30.54 m below land surface.

autooscillation of air, (2) diurnal fluctuations due to gravitational effects and warming and cooling of air caused by the daily alternation of solarization, (3) longer term fluctuations on the order of days to weeks due to weather and frontal systems as they move across the earth's surface, and (4) annual fluctuations due to seasonal warming and cooling of the atmosphere [*Massmann and Farrier*, 1992; *Ahlers et al*., 1999; *Gebert and Groengroeft*, 2006; *Wu et al*., 2006]. When considering subsurface airflow and gas transport, the two most important kinds of fluctuations are diurnal fluctuations and fluctuations associated with weather patterns [e.g., *Martinez and Nilson*, 1999].

[5] The autooscillation of air, detected at a resolution of 10 min, induces atmospheric pressure fluctuations of less than 0.1 kPa, which always underlie the greater pressure fluctuations [*Gebert and Groengroeft*, 2006]. The thermal and gravitational effects induced diurnal atmospheric pressure fluctuations are on the order of a few millibars (1 mbar = 0.1 kPa) [*Massmann and Farrier*, 1992]. The fluctuations induced by variations in weather patterns are much larger than the diurnal thermal and gravitational effects and are on the order of tens of millibars [*Massmann and Farrier*, 1992]. *Massmann and Farrier* [1992] observed that the atmospheric pressure at Houghton, Michigan, during a snowstorm in December 1989 and during a mild rainstorm in July 1990 changed by 2–3 kPa during a 24 h period. *Ellerd et al*. [1999] observed that the mean atmospheric pressure at the Hanford nuclear reservation near Richland, Washington, is approximately 98.7 kPa, and typical atmospheric pressure fluctuations resulting from large-scale weather patterns are on the order of 1 kPa [*Rohay*, 1996]. *Nilson et al*. [1991] stated that the amplitudes of the cyclical variations in atmospheric pressure caused by weather patterns are on the order of 1–3 kPa over periods of a few days.

[6] Observations show that atmospheric pressure differs by at least 0.5 kPa from the mean pressure over 50% of the time. For the Lake Superior region, atmospheric pressure data collected from 1960 to 1973 show that the mean pressure during this 13 year period is 101.5 kPa and more than 50% of the data differ by at least 0.5 kPa from the mean pressure [*Massmann and Farrier*, 1992]. In Karup, Denmark, the mean atmospheric pressure during the period from 1953 to 1995 was 101.37 kPa, and the pressure differed by at least 0.5 kPa from the mean more than 60% of the time [*Elberling et al*., 1998]. The atmospheric pressure in 1993 changed in cycles that deviated up to 3 kPa from the mean [*Elberling et al*., 1998].

[7] The spatial gradients of atmospheric pressure are generally quite small relative to the temporal gradients [*Massmann and Farrier*, 1992]. In general, spatial gradients in atmospheric pressure rarely exceed 0.3 kPa per 100 km [*Miller and Thompson*, 1970]. Hence, the atmospheric pressure at the local or site scale can be assumed unsteady but uniform [*Massmann and Farrier*, 1992].

2.2. Propagation of Atmospheric Pressure Fluctuations Into the Subsurface

[8] The fluctuations of atmospheric pressure induce the fluctuations of air pressure in the subsurface [*Ahlers et al*., 1999]. The propagation of air pressure into the subsurface was first described and analyzed by *Buckingham* [1904]. An analytical solution was developed to determine the air pressure at any depth in response to periodic atmospheric pressure fluctuation at the ground surface. However, the pressure fluctuations are observed to propagate with time delay and amplitude attenuation [*Buckingham*, 1904; *Weeks*, 1979, 1987; *Rossabi et al*., 1993; *Ahlers et al*., 1999; *Downs et al*., 2000; *Lu and Likos*, 2004; *Wu et al*., 2006]. The degree of time delay and amplitude attenuation depend on the unsaturated zone structure and air permeability. Observations of atmospheric pressure changes and subsurface air pressure responses abound in the literature [*Nilson et al*., 1991; *Pirkle et al*., 1992; *Rohay et al*., 1993; *Rossabi et al*., 1993; *Rossabi and Riha*, 1994; *Shan*, 1995; *Rohay*, 1996; *Stephens*, 1996; *Elberling et al*., 1998; *Ahlers et al*., 1999; *Ellerd et al*., 1999; *Olson et al*., 2001; *Tillman et al*., 2001; *Rossabi and Falta*, 2002; *Riha*, 2005; *Wu et al*., 2006].

[9] An example of these observations is shown in Figure 1. The experimental method for obtaining the data is described in *Rossabi and Riha* [1994]. Figure 1 shows that the fluctuation of the pressures is nearly periodic. The fluctuation of the atmospheric pressure is characterized by two cyclic signals of different frequencies and amplitudes. The larger amplitude, lower frequency pressure cycle has a period of approximately 5 days and is caused by weather fronts passing through the experimental site [*Rossabi and Falta*, 2002]. The smaller amplitude, higher frequency pressure cycle is due to the diurnal solar heating and cooling patterns. *Rossabi and Falta* [2002] observed similar pressure patterns at all the observation locations. Figure 1 also shows that the response of the subsurface pressure to the surface pressure is significantly damped and lagged. The subsurface air pressure at a depth of 30.54 m lags the surface pressure by approximately 12 h. It is believed that the time delay is caused by the compressibility of the gas and the resistance to flow imposed by the permeable medium [*Weeks*, 1987; *Rossabi and Falta*, 2002].

[10] The fluctuations of the atmospheric pressure induce gas movement between the atmosphere and the subsurface. Gas movement in the unsaturated zone induced by natural fluctuations in atmospheric pressure is referred to as barometric pumping or atmospheric pumping [*Nilson et al*., 1991; *Pirkle et al*., 1992; *Auer et al*., 1996; *Elberling*

et al., 1998; *Rossabi et al*., 1998; *Riha*, 2005; *You et al*., 2010, 2011; *Li et al*., 2012a]. When the atmospheric pressure falls, gases are drawn upward out of the subsurface into the atmosphere. Conversely, when the atmospheric pressure increases, fresh air is pushed downward into the subsurface [*Buckingham*, 1904; *Nilson and Lie*, 1990; *Nilson et al*., 1991; *Pinault and Baubron*, 1997; *Gebert and Groengroeft*, 2006]. Generally, the fluctuations of atmospheric pressure increases soil-atmosphere gas exchange [*Poulsen and Sharma*, 2011].

[11] In a homogeneous porous medium, the depth of the propagation of air pressure into the subsurface can be from several meters to over 10 m. On the basis of numerical analyses, *Massmann and Farrier* [1992] concluded that fresh air can migrate several meters into the subsurface during a typical atmospheric pressure cycle. *Auer et al*. [1996] calculated that the atmospheric pressure change propagates to a depth over 10 m for moderately permeable materials. *Parker* [2003] believed that atmospheric pressure fluctuations may be expected to propagate to significant depths in soils that are at least moderately permeable. *Tillman and Smith* [2005] found that the soil gas movement reaches a depth of more than 2.5 m in a 3 m deep unsaturated zone in response to natural changes in atmospheric pressure and additional simulations show deeper air movement for deeper unsaturated zones.

[12] In a heterogeneous system, with low permeable layers at the surface or in the vadose zone or the system is a fractured rock system, the propagation of gas pressure into the subsurface may be much greater [*Nilson et al*., 1991; *Elberling et al*., 1998]. Horizontal gas pressure gradients can develop at sites with near-surface heterogeneities. These gradients may cause fresh air to intrude meters or tens of meters into the unsaturated zone during a storm event [*Massmann and Farrier*, 1992]. *Elberling et al*. [1998] carried out field study and numerical analysis in a glacial aquifer with 10–12 m thick sandy unsaturated zone to investigate gas exchange between the atmosphere and the unsaturated zone. The investigation shows that during an atmospheric pressure cycle, atmospheric oxygen was observed to migrate more than 10 m/d horizontally in the capped (covered by a low-permeability layer) unsaturated zone. The analysis also shows that the combination of the effects of amplitude and the length of the period of atmospheric pressure variations determine the extent of a unsaturated zone where atmospheric oxygen can reach. *Tillman and Smith* [2005] concluded from numerical analyses that airflow was increased in a two-layered unsaturated zone with a low-permeability layer on the top compared with the airflow in a single-layer unsaturated zone.

[13] In a fractured permeable medium, the open fractures and permeable faults will generally serve as breathing passages, greatly increasing the amplitude and nonuniformity of vertical gas motions and permit atmospheric pressure fluctuations to propagate deep into the ground [*Nilson et al*., 1991; *Auer et al*., 1996; *Wu et al*., 2006]. *Shan et al*. [1999] stated that a highly permeable leaky fault could provide a preferred pathway for subsurface gas flow. *Ahlers et al*. [1999] used one-dimensional, two-dimensional, and three-dimensional models to simulate the measured subsurface air pressure responses at Yucca Mountain, Nevada. Results show that faults are fast pathways for gas flow and a transient gas pulse will be transmitted almost entirely through the fracture. At the Nevada Test Site, in situ pressure measurements indicate that oscillatory gas motions induced by fluctuations of atmospheric pressure reach all the way down to the water table (about 400 m) in geological formations consisting of either alluvium or fractured volcanic rock [*Nilson and Lie*, 1990]. *Montazer et al*. [1988] detected responses to short-term atmospheric pressure fluctuations in the borehole in Yucca Mountain to a maximum depth of about 91 m and only responses to long-term fluctuations were detectable below this depth. On the basis of a theoretical analysis, *Nilson et al*. [1991] stated that the transport of contaminant gas by barometric pumping in the fracture may be orders of magnitude more significant than molecular diffusion.

2.3. Single-Phase Airflow Model

[14] Theoretical analysis of single-phase airflow in subsurface porous media is based on the following assumptions [*Kidder*, 1957]: (1) the flow of gas follows Darcy's law, (2) the only phase flowing is a gas of constant composition and viscosity, (3) the gas is an ideal gas, (4) the porous medium is homogeneous and isotropic, and (5) gravitational and thermal effects are neglected.

[15] The governing equation for single-phase airflow can be developed from Darcy's law and the principle of mass conservation. In general problems, the gravitational and temperature effects can be safely ignored [*Scanlon et al*., 2002; *Lu and Likos*, 2004]. For isothermal one-dimensional transient vertical airflow in homogeneous and isotropic porous medium, the general governing equation can be written as [*Kidder*, 1957; *Massmann*, 1989]

$$\frac{\partial p_a}{\partial t} = \frac{k_a}{\phi_a \mu_a} \frac{\partial}{\partial z}\left(p_a \frac{\partial p_a}{\partial z}\right) \tag{1}$$

where p_a is the air pressure, t is the time, z is the vertical coordinate, k_a is the air permeability, ϕ_a is the air-filled porosity, and μ_a is the air viscosity. Equation (1) can also be written as [*Kidder*, 1957; *Katz et al*., 1959]

$$\frac{\partial p_a^2}{\partial t} = \alpha \frac{\partial^2 p_a^2}{\partial z^2} \tag{2}$$

where α is the pneumatic diffusivity (air diffusivity) and is defined as

$$\alpha = \frac{k_a p_a}{\phi_a \mu_a} \tag{3}$$

[16] The dependent variable of equation (2) is p_a^2. Equation (2) is a nonlinear partial differential equation because the pneumatic diffusivity α depends on the air pressure p_a. In order to linearize equation (2), the mean atmospheric pressure p_{a0} is used instead of p_a in the pneumatic diffusivity term [e.g., *Fukuda*, 1955; *Kidder*, 1957; *Weeks*, 1978; *Massmann*, 1989; *Shan*, 1995; *Wu et al*., 1998; *Lu*, 1999; *Neeper*, 2002; *Massman*, 2006; *You et al*., 2011; *Li et al*., 2012a]. It can be seen from the section 2.2 that the magnitude of the atmospheric pressure fluctuation is less than 10% of the mean pressure. Therefore, the linearization will

not cause significant error [*Massmann*, 1989; *Massmann and Farrier*, 1992; *Shan*, 1995; *Lu*, 1999; *Lu and Likos*, 2004]. For problems in which the air pressure varies only slightly from the mean pressure, a second approximation to equation (2) can be obtained [*Fukuda*, 1955; *Weeks*, 1978; *Massmann*, 1989; *Scanlon et al*., 2002]

$$\frac{\partial p_a}{\partial t} = \alpha \frac{\partial^2 p_a}{\partial z^2} \tag{4}$$

Equation (4) is a linear differential equation with p_a as the dependent variable.

[17] The equation for three-dimensional airflow in homogeneous and isotropic porous media is given by *Kirkham* [1947] and *Muskat* [1946]. In heterogeneous and anisotropic porous media, the corresponding governing equation can be found in *Bear* [1972] and *Lu and Likos* [2004].

[18] Equations (3) and (4) are diffusion equations, and some of the solutions are readily available in *Carslaw and Jaeger* [1959]. The fluctuations of atmospheric pressure at the ground surface can either be assumed to be sinusoidal fluctuations [e.g., *Buckingham*, 1904; *Farrell et al*., 1966; *Purtymun et al*., 1974; *Rojstaczer and Tunks*, 1995; *Ahlers et al*., 1999; *Tillman et al*., 2001; *Lu and Likos*, 2004] or arbitrary functions [e.g., *Shan*, 1995; *Lu*, 1999; *Lu and Likos*, 2004; *You et al*., 2011; *Li et al*., 2012a].

[19] The propagation of air pressure into an infinitely deep porous medium was investigated by a number of researchers [*Fukuda*, 1955; *Hanks and Woodruff*, 1958; *Farrell et al*., 1966; *Wigley*, 1967; *Clements and Wilkening*, 1974; *Purtymun et al*., 1974; *Clarke et al*., 1987; *Clarke and Waddington*, 1991; *Ishihara et al*., 1992; *Ahlers et al*., 1999; *Neeper*, 2002, 2003; *Perrier and Richon*, 2010]. Equation (4) was used as the governing equation in all these studies. *Kidder* [1957] derived analytical solutions for the propagation of air pressure into infinite porous medium using both equations (1) and (2). In the derivation of the solutions, the air pressure at infinitely depth was set to be a finite value.

[20] The propagation of air pressure into finite depth porous medium was first studied analytically by *Buckingham* [1904]. *Kirkham* [1947] considered a soil sample with a specified length and presented an analytical solution for predicting the air pressure in the sample in response to the air pressure change at the sample surface. The propagation of air pressure into the subsurface bounded below by a water table or an impervious boundary was studied by many researchers [*Farrell et al*., 1966; *Kimball and Lemon*, 1972; *Colbeck*, 1989; *Nilson et al*., 1991; *Ishihara et al*., 1992; *Cunningham and Waddington*, 1993; *Rojstaczer and Tunks*, 1995; *Auer et al*., 1996; *Tillman et al*., 2001; *Rossabi and Falta*, 2002; *Lu and Likos*, 2004; *Massman*, 2006; *Perrier and Richon*, 2010; *You et al*., 2011]. The water table was assumed to be static and impermeable at which a no-flow boundary was assigned. *Abbas* [2011] derived an analytical solution to account for the water table fluctuations. Equation (4) was chosen as the governing equation in these investigations. In addition, researchers also used equation (2) to derive analytical solutions for the propagation of pressure into finite depth porous medium bounded below by a water table [*Shan*, 1995; *Lu*, 1999; *Li et al*., 2012a].

2.4. Airflow to a Barometric Pumping Well

[21] When atmospheric pressure changes, airflow can be induced in an open borehole or a well screened in the unsaturated zone. The airflow between the subsurface and the well depends on the air pressure difference between the air pressure in the well and the air pressure in the surrounding porous media [*You et al*., 2010]. Such a well is referred to as a barometric pumping well [*You et al*., 2010, 2011]. Observers have long noted that open wells "breathe" in response to atmospheric pressure fluctuations, i.e., to inhale ambient air and exhale soil gas to the atmosphere [*Fairbanks*, 1896; *Ferris et al*., 1962; *Purtymun et al*., 1974; *Woodcock and Friedman*, 1979; *Weeks*, 1987; *Woodcock*, 1987; *Rohay et al*., 1993; *Foor et al*., 1995; *Thorstenson et al*., 1998].

[22] Analytical solutions were derived for airflow to a barometric pumping well by a number of researchers [*Rossabi and Falta*, 2002; *Neeper*, 2003; *You et al*., 2011]. The solution presented by *Rossabi and Falta* [2002] is the first analytical solution for subsurface airflow to a barometric pumping well induced by surface atmospheric pressure fluctuations. In the derivation of the solution, the airflow rate was approximated by a decomposition method. Using the same method, *Neeper* [2003] presented a harmonic analysis of airflow in open boreholes due to barometric pressure changes. Following the work of *Rossabi and Falta* [2002] and *Neeper* [2003], *You et al*. [2011] derived a semianalytical solution for determining the time-dependent gas flow rates to and from a barometric pumping well in a multilayer unsaturated zone. The error induced by the decomposition method [*Rossabi and Falta*, 2002; *Neeper*, 2003] was also investigated by *You et al*. [2011].

[23] The decomposition method includes two steps. The first step is to calculate the subsurface air pressure without the barometric pumping well from the one-dimensional vertical airflow equation in response to surface atmospheric pressure fluctuations. The second step is to use the obtained subsurface air pressure as the background pressure to calculate the one-dimensional horizontal airflow to and from the barometric pumping well [*You et al*., 2011]. Equation (4) is chosen as the governing equation for the one-dimensional vertical airflow. For the one-dimensional horizontal radial airflow, the following equation [*Wigley*, 1967; *Rossabi and Falta*, 2002] is chosen as the governing equation

$$\frac{1}{\alpha_r}\frac{\partial p_a}{\partial t} = \frac{\partial^2 p_a}{\partial r^2} + \frac{1}{r}\frac{\partial p_a}{\partial r} \tag{5}$$

where r is the radial distance from the barometric pumping well and α_r is the radial air diffusivity and can be written as

$$\alpha_r = \frac{k_{ar} p_{a0}}{\phi_a \mu_a} \tag{6}$$

in which k_{ar} is the air permeability in the r direction. Equation (5) is a linearized equation with p_a as the dependent variable. The equation with p_a^2 as the dependent variable is given by *Katz et al*. [1959].

[24] The decomposition method is an approximate method and researchers attempted to derive more physically based two-dimensional or three-dimensional models.

The governing equation for two-dimensional transient airflow to a barometric pumping well, for example, is given by *Falta* [1996]. *Ellerd et al*. [1999] presented a two-dimensional numerical investigation of airflow in a three layer unsaturated zone at the Hanford site. *You et al*. [2010] first derived a two-dimensional semianalytical solution for airflow to a barometric pumping well. In the solution, the well can be either with or without a check valve.

2.5. Applications of Induced Airflow

2.5.1. Air Permeability Estimation

[25] Air permeability of soils is an important parameter to many science and engineering fields, such as soil and agriculture sciences, chemical and petroleum engineering, hydrology, and environmental engineering [*Springer et al*., 1995; *Dury et al*., 1999; *Shan et al*., 1999]. Air permeability and pneumatic diffusivity can be determined from the response of subsurface air pressure to surface atmospheric pressure fluctuations [*Scanlon et al*., 2002]. The air permeability is determined by matching the calculated subsurface air pressure to the observed data.

[26] *Stallman* [1967] first suggested the using of air pressure difference between the surface and subsurface to calculate the permeability of unsaturated zone material. *Stallman and Weeks* [1969] computed hydraulic conductivity of the unsaturated zone using the atmospherically induced gas pressure fluctuations. On the basis of *Stallman*'s [1967] work, *Weeks* [1978] applied a numerical approach to determine the vertical air permeability of layered materials. *Rojstaczer and Tunks* [1995] conducted a field test and derived a one-dimensional analytical solution to determine the air diffusivity of a shallow, layered soil system. Air permeabilities were then determined using measured porosity and calculated air diffusivity. *Shan* [1995] derived analytical solutions for the determination of vertical air permeability of single-layered and multilayered unsaturated soils using observed air pressure data at the land surface and at depth in the unsaturated zone. *Shan et al*. [1999] derived analytical solutions for determining air permeability of leaky faults in the vadose zone. *Lu* [1999] and *Lu et al*. [2001] used time series Fourier analysis method to predict subsurface air pressure response and to determine the vertical air permeability. *Rossabi and Falta* [2002] used a time step function to deal with the atmospheric pressure data and derived a simplified analytical solution for calculating subsurface air pressure and for determining air permeability. *Li et al*. [2012a] developed an analytical solution to determine the vertical air permeabilities of a three-layer unsaturated zone. *Wu et al*. [2006] presented a three-dimensional modeling study of gas flow to estimate the large-scale fracture permeability of the Yucca Mountain unsaturated zone using atmospheric pressure data. *Olson et al*. [2001] compared different methods (laboratory experiments, field air pumping tests, and the method presented herein) for determining air permeability and found that all the three methods give similar results at Picatinny Arsenal, New Jersey.

2.5.2. Passive Soil Vapor Extraction

[27] Passive soil vapor extraction (PSVE) refers to the enhancement and application of the open-well natural breathing phenomenon as a remediation method for increased VOCs removal rates from the unsaturated zone [*Rohay et al*., 1993]. It relies on atmospheric pressure fluctuations to pump soil gas out of the well [*Rohay*, 1996]. PSVE is a complementary technology to be used with active soil vapor extraction (ASVE) [*Rohay et al*., 1993]. The flow rates for a typical well in PSVE systems are generally low compared to ASVE [*Riha*, 2005]. The primary advantages of PSVE are minimal operating and maintenance costs [*Rohay et al*., 1993; *Rossabi and Falta*, 2002; *Jennings and Patil*, 2002; *Riha*, 2005; *Kamath et al*., 2009]. PSVE can be used to clean up the zones of low VOC concentration, the zones of limited mass transfer or remote sites, or sites where a long-term remedial technology is acceptable.

[28] A PSVE system involves a well that is screened in the unsaturated zone and open to the atmosphere [*Ellerd et al*., 1999]. The passive breathing is driven primarily by the difference between the atmospheric pressure and the subsurface soil gas pressure near the well openings. Gas flows out of the subsurface through the open well when the subsurface gas pressure is greater than atmospheric pressure and into the subsurface through the open well when the subsurface gas pressure is smaller. The gas that enters the subsurface is typically free of contaminants. Hence, the result of PSVE is a net flow of contaminants out of the subsurface [*Ellerd et al*., 1999].

[29] The efficiency of PSVE can be enhanced by gas filters, check valves, and surface covers [*Rossabi and Riha*, 1994; *Rohay*, 1996; *Rossabi et al*., 1998; *Ellerd et al*., 1999; *Downs et al*., 2000; *Riha*, 2005]. *Rossabi and Riha* [1994] found that one-way valves on wells (allowing airflow out of the well only) can increase contaminant removal by at least a factor of two. *Ellerd et al*. [1999] evaluated numerically the effectiveness of these enhancements at a site contaminated with carbon tetrachloride at the Hanford nuclear reservation. Simulation results show that the volumetric flow rates are more than doubled with surface covers up to 90 m radius. Results by *Ellerd et al*. [1999] also show that check valves might increase the subsurface gas extraction rate by a factor of nearly three.

[30] PSVE has been successfully applied to contaminated site remediation and has been field tested as an effective remediation technology. Large chlorinated VOCs removal rate as much as 1–2 kg/d was observed in each well at the Savannah River Integrated Demonstration Site by *Rossabi et al*. [1993]. At the Savannah River Site, more than 23 kg of chlorinated solvent was removed during the first year of operation [*Rossabi et al*., 1998]. An observation made by *Christensen et al*. [2000] revealed that a total air volume of 300 m^3 and a total mass of 45 g chlorinated solvents have been passively extracted during a 10 day period. *Downs et al*. [2000] observed that the flow rates by PSVE varied from 50 L/d for a single well at one site to 68,000 L/d at another. A total of 62.033 kg of VOCs were removed in 1998 and a total of 102.517 kg of VOCs were removed in 1999 at the tested sites. At the Metallurgical Laboratory Site, approximately 122.47 kg of chlorinated organic contaminants have been removed from the wells fitted with BaroBall valves after 7 years of PSVE operation [*Riha*, 2005].

[31] PSVE can be applied to any site where volatile contaminants (chlorinated solvents, petroleum products, etc.) have contaminated the vadose zone [*Rossabi et al*., 1998].

However, the performance of this technology is very sensitive to site geology [*Ellerd et al*., 1999]. The sites well suited for PSVE are those with thick unsaturated zones or low-permeability layers that increase the damping and delay of the atmospheric pressure fluctuation signal [*Rossabi et al*., 1998, *Christensen et al*., 2000]. The low-permeability layers can be natural or artificial surface covers [*Massmann and Farrier*, 1992; *Ellerd et al*., 1999].

2.5.3. Passive Bioventing

[32] The natural air exchange between surface and subsurface induced by atmospheric pressure fluctuations can also be applied to the passive bioventing technology. Passive bioventing is the use of the natural air exchange to aerate subsurface soils to stimulate in situ biological activity and promote bioremediation [*Foor et al*., 1995; *Larson and Hoeppel*, 2004]. Bioventing is designed to maximize biodegradation of aerobically biodegradable compounds, with some volatilization occurring [*Foor et al*., 1995]. Passive bioventing system is effective in aerating petroleum-contaminated, oxygen-limited soils [*Foor et al*., 1995]. Passive bioventing could reduce costs compared with bioventing and may be an attractive alternative for remote sites [*Foor et al*., 1995; *Zimmerman et al*., 2003; *Larson and Hoeppel*, 2004]. The primary advantage of passive bioventing is to eliminate the need for an electrically powered blower. The primary disadvantage of passive bioventing is that it is only applicable to sites with a sustained difference between atmospheric pressure and subsurface gas pressure [*Zimmerman et al*., 2003; *Larson and Hoeppel*, 2004; *Larson*, 2006].

2.5.4. Radon Transport

[33] Radon is a very important gas in soil because of its potential health hazards [e.g., *Schery and Gaeddert*, 1982; *Nazaroff*, 1992; *Tung et al*., 2013]. Atmospheric pressure fluctuations have been found to cause significant changes in soil-gas radon concentrations. During periods of decreasing atmospheric pressure, soil gas is drawn from the ground, which may increase the radon concentration in the near-surface soil layers. During periods of increasing atmospheric pressure, atmospheric air free of radon is forced into the ground, which may decrease the radon concentration in the upper soil layers and drive radon deeper into the soil [*Kovach*, 1945; *Kraner et al*., 1964; *Clements and Wilkening*, 1974; *Lindmark and Rosen*, 1985; *Schumann et al*., 1992; *Holford et al*., 1993]. The pattern of lowering pressure/rising radon and rising pressure/lowering radon has been observed by many researchers [*Kovach*, 1945; *Moses et al*., 1963; *Pohl-Rüling and Pohl*, 1969; *Schery et al*., 1982, 1984; *Schumann et al*., 1992; *Chen et al*., 1995; *Pinault and Baubron*, 1996; *Eff-Darwich et al*., 2002; *Perrier et al*., 2004; *Sundal et al*., 2008; *Perrier and Richon*, 2010; *Zoran et al*., 2012]. Soil radon concentrations at different depths in response to atmospheric pressure changes have also been presented [*Kraner et al*., 1964; *Schery et al*., 1984].

[34] A change in atmospheric pressure causes a pressure gradient between the atmosphere and soil, which induces vertical gas transport [*Schumann et al*., 1992]. The radon flux at the ground surface is expected to increase during a falling atmospheric pressure, due to both the "piston withdrawal" of the surface soil gas layer and the increased radon gradient in the surface layers [*Kraner et al*., 1964; *Tanner*, 1964; *Schery et al*., 1989; *Holford et al*., 1993]. On the other hand, the radon flux from the soil surface to the atmosphere is expected to decrease during an increasing atmospheric pressure [*Holford et al*., 1993; *Koarashi et al*., 2000]. *Holford et al*. [1993] found that the decrease in radon flux density caused by rising atmospheric pressure is smaller than the increase in radon flux density caused by falling atmospheric pressure by the same magnitude. Therefore, periods of alternately rising and falling atmospheric pressure show a net enhancement of radon flux. *Schery et al*. [1984] found that atmospheric pressure changes mainly affect the instantaneous exhalation of radon and the effect on time-averaged radon exhalation is small.

[35] The radon flux at the ground surface can vary from 10% to as much as a factor of 2 due to atmospheric pressure changes. *Clements and Wilkening* [1974] observed that atmospheric pressure changes of 1–2% associated with the passage of weather fronts could produce changes in the radon flux from 20% to 60%, depending upon the rate of pressure change and its duration. *Schery and Gaeddert* [1982] concluded from observation data that atmospheric pressure change induced a mean enhancement in radon flux of about 10%. In an abandoned mine in Socorro Peak, Socorro, New Mexico, *Schery et al*. [1982] concluded that the natural atmospheric fluctuation caused an enhancement factor of 2 in the radon flux. *Schery and Petschek* [1983] found that rising and falling atmospheric pressure provided major changes in radon exhalation, consistent with the findings of *Clements and Wilkening* [1974]. Measurements carried out by *Schery et al*. [1984] at a site about 1 km west of the center of the New Mexico Institute of Mining and Technology campus indicate that instantaneous exhalation of radon could easily vary by a factor of 2 or more due to atmospheric pressure changes.

[36] Various models have been developed to interpret the effects of atmospheric pressure changes on radon transport from soil to atmosphere. The two major components of radon migration are diffusion and advection [*Tanner*, 1964; *Klusman and Jaacks*, 1987; *Nazaroff*, 1992]. Some researchers used pure diffusion models to simulate the radon transport process [e.g., *Kraner et al*., 1964; *Tanner*, 1964; *Nazaroff*, 1992]. However, field data show that variations in radon concentrations are larger than that predicted from pure diffusive transport alone [*Kraner et al*., 1964; *Schery et al*., 1982; *Hutter*, 1996]. Hence, models including both diffusion and advection were developed. *Clements and Wilkening* [1974] presented the first analytical investigation of the effects of atmospheric pressure changes on radon transport across the earth-air interface considering both diffusion and advection. In their model, the velocity field is assumed to be induced by atmospheric pressure only and reasonable fit is obtained between experimental and theoretical data. *Edwards and Bates* [1980] developed a model to calculate radon flux results from arbitrary atmospheric pressure changes in a composite system. *Schery et al*. [1982] developed models for transport of radon from fractured rock considering atmospheric pressure variations. *Schery and Siegel* [1986] developed models to investigate the effect of channels on the transport of radon from soil to air. *Holford et al*. [1993] presented a two-dimensional finite element code to model radon transport in

cracked dry soil. *Pinault and Baubron* [1997] presented a one-dimensional model to calculate the response of soil gas radon concentration to diurnal and semidiurnal atmospheric pressure changes and to estimate soil gas transport parameters. *Eff-Darwich et al*. [2002] developed a model based on the assumption that radon is transported by molecular diffusion combined with atmospheric pressure induced advective flow and used the model to interpret the measured radon data in galleries of a volcanic island. Well-documented numerical simulators are also available to simulate the transport of radon in response to atmospheric pressure changes, such as Rn3D [*Holford*, 1994], LEACHV [*Chen et al*., 1995], and RnMod3d [*Andersen*, 2000].

[37] Although a clear relationship has been found between radon flux and atmospheric pressure, conflicting results exist in the literature regarding the effects of atmospheric pressure changes on fluctuation in radon flux and concentration [e.g., *Moses et al*., 1963; *Guedalia et al*., 1970; *Fleischer and Mogro-Campero*, 1979; *Schubert and Schulz*, 2002; *Richon et al*., 2004; *Perrier et al*., 2007; *Steinitz et al*., 2007; *Richon et al*., 2009]. *Fleischer and Mogro-Campero* [1979] observed enhancements in radon flux during both decreasing and increasing atmospheric pressures. On the basis of measurements of radon concentration in a column under well-defined conditions, *Schubert and Schulz* [2002] concluded that there is no impact of atmospheric pressure variations on radon migration and the atmospheric pressure leads to long-term changes in radon concentration rather than diurnal alterations. In addition, both positive [*Galmarini*, 2006] and negative [*Klusman and Jaacks*, 1987; *Schery et al*., 1989; *Hutter*, 1996; *Iakovleva and Ryzhakova*, 2003; *Smetanová et al*., 2010] correlations between radon concentration and atmospheric pressure were found. Some researchers stated that only sudden drops or increases of atmospheric pressure (of the order of 1.0–1.5 kPa) can affect the radon exhalation [*Kataoka et al*., 2003; *Galmarini*, 2006]. Due to the fact that several meteorological parameters (e.g., atmospheric pressure, wind, precipitation, and temperature) may change simultaneously, the determination of the relative influence of atmospheric pressure changes on radon migration and soil gas radon concentration is difficult [*Tanner*, 1964; *Schumann et al*., 1992].

2.5.5. Carbon Dioxide Transport

[38] Atmospheric pressure fluctuations have also been found to have a significant effect on transport of CO_2 from soil to atmosphere [*Massman et al*., 1995; *Massman*, 2006]. When atmospheric pressure at the ground surface is lower than the average atmospheric pressure, more CO_2 will seep out of the ground surface; when the atmospheric pressure at the ground surface becomes larger than the average atmospheric pressure, pure air without CO_2 will flow back into the subsurface [*Zhang et al*., 2004]. Increasing atmospheric pressure decreases the CO_2 fluxes and vice versa [*Christophersen et al*., 2001]. At an old landfill, *Christophersen et al*. [2001] found that increasing the atmospheric pressure decreases the CO_2 flux out of the soil due to a decreasing pressure gradient between the landfill and the atmosphere. *Baldocchi and Meyers* [1991] observed enhanced CO_2 flux induced by atmospheric pressure fluctuations above the floor of a deciduous forest. Many researchers found that there is a negative correlation between atmospheric pressure and soil CO_2 efflux [*Chiodini et al*., 1998; *Christophersen et al*., 2001; *Rogie et al*., 2001; *Granieri et al*., 2003; *Viveiros et al*., 2008, 2009]. *Hinkle* [1994] found that a decrease of approximately 0.5 cm atmospheric pressure caused decreases in CO_2 concentration of approximately 0.03% and 0.05% at 1.2 and 2.0 m depths, respectively.

[39] The transport of CO_2 from soil to atmosphere is through both diffusion and advection [*Baver et al*., 1972; *Massman et al*., 1995, 1997; *Luo and Zhou*, 2006; *Massman*, 2006]. *Massman et al*. [1995, 1997] developed one-dimensional steady state diffusion and one-dimensional and three-dimensional time-dependent pressure pumping (advection) models to estimate CO_2 fluxes through snowpack. *Massman* [2006] derived an analytical model for advective transport of CO_2 in a two-layered permeable media (snowpack and soil) induced by atmospheric pressure fluctuations.

[40] Similar to radon, conflicting results also exist for the effect of atmospheric pressure changes on the transport of CO_2 from soil to atmosphere [*McGee and Gerlach*, 1998; *McGee et al*., 2000; *Lewicki et al*., 2003, 2007, 2008; *Subke et al*., 2003; *Massman and Frank*, 2006; *Viveiros et al*., 2008]. On the basis of observation data, *Lewicki et al*. [2003] concluded that surface wind, not barometric pumping, is the main driving force for advective soil gas flow over diurnal cycles. Similar results were also found by *McGee et al*. [2000] and *Viveiros et al*. [2008]. *Massman and Frank* [2006] found that the atmospheric forcing is possibly a mixture of pressure changes and wind speed variations and the wind speed is a better measure of advective forcing than is the atmospheric pressure changes. *Lewicki et al*. [2007, 2008] observed positive correlation between CO_2 discharge and average daily atmospheric pressure and found that average daily CO_2 discharge was correlated with both average daily wind speed and atmospheric pressure. *Lewicki et al*. [2007] concluded that atmospheric pressure cannot exert a strong influence on average daily CO_2 emissions. *Subke et al*. [2003] stated that atmospheric pressure fluctuations only affect the instantaneous CO_2 efflux and the net contribution of the pressure related transport would be zero when averaged over time.

2.5.6. Water Vapor Transport

[41] Water vapor is the most important component of gas exchange at the Earth-atmosphere interface from a hydrological perspective [*Nachshon et al*., 2012]. Subsurface water vapor may be removed as a result of atmospheric pressure fluctuations at the land surface [*Tsang and Pruess*, 1989]. When atmospheric pressure increases, air with low relative humidity is forced into the formation. The incoming dry air will be humidified by mixing with soil gas and by evaporation of soil moisture. When atmospheric pressure decreases, the gas with higher humidity will be discharged back to the atmosphere. Because the outgoing gas has a higher relative humidity than the incoming gas, thus atmospheric pressure fluctuations caused water vapor transport from soil to atmosphere [*Tsang and Pruess*, 1989; *Martinez and Nilson*, 1999].

[42] Fluctuations in atmospheric pressure have been found to have a significant influence on the transfer of water vapor [*Cary*, 1967; *Kimball and Lemon*, 1971; *Baldocchi and Meyers*, 1991; *Ishihara et al*., 1992; *Martinez*

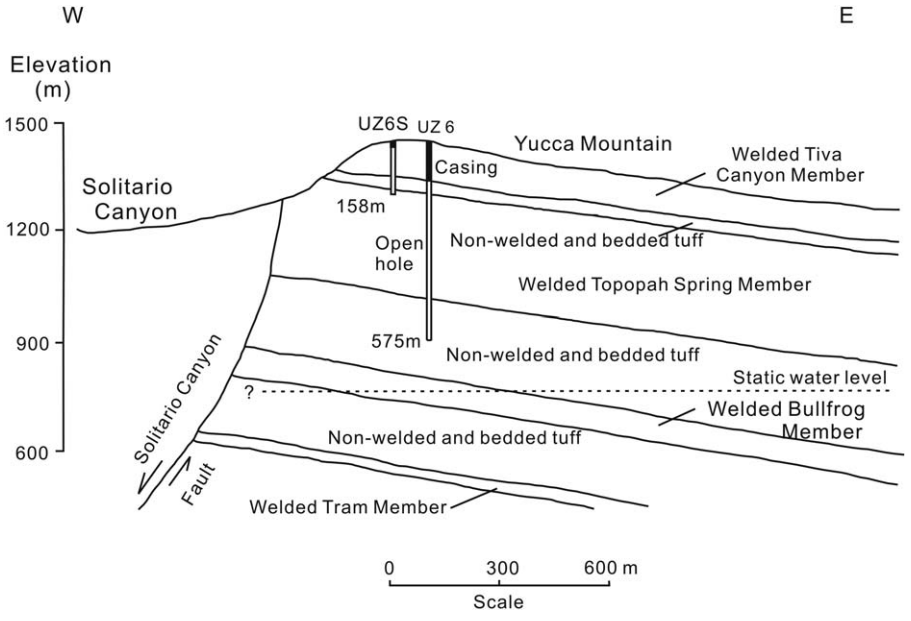

Figure 2. Generalized cross section of Yucca Mountain at the sites of wells UZ6 and UZ6S (modified from *Weeks* [1987]).

and Nilson, 1999]. *Kimball and Lemon* [1971] concluded that fluctuations in air pressure can significantly increase the evaporation of water through coarse mulches or through very shallow depths of soils. *Baldocchi and Meyers* [1991] observed that atmospheric pressure fluctuations enhance the efflux of water vapor from the wet litter of a deciduous forest. In a cylindrical soil column, *Cary* [1967] observed that an increase in ambient pressure decreases the evaporation rate and a decrease in ambient pressure increases the evaporation rate. *Cary* [1967] also observed that the evaporation responds quickly to changes in the ambient pressure. Barometric pumping can also cause venting of soil moisture from matrix into fracture in fractured media [*Weisbrod and Dragila*, 2006], and the mechanism of surface efflux of water vapor from fractured media driven by barometric pumping was presented by *Martinez and Nilson* [1999]. It has been found that the transport of water vapor by barometric pumping from depth of a fractured medium is an order of magnitude greater than the vertical water vapor flux carried from depth by diffusion [*Martinez and Nilson*, 1999]. On the other hand, *Scanlon and Milly* [1994] stated that the long-term impact of barometric pumping on water vapor movement is relatively minor.

[43] The influence of atmospheric pressure fluctuations on water vapor transport has been studied theoretically for a long time. Some researchers assumed sinusoidal atmospheric pressure changes at the ground surface and derived analytical solutions to predict the gas flux [*Fukuda*, 1955; *Farrell et al*., 1966; *Scotter and Raats*, 1969]. *Ishihara et al*. [1992] assumed the fluctuating atmospheric pressure to be statistically homogeneous and steady at the ground surface and can be represented by a Fourier integral and derived an analytical model. *Tsang and Pruess* [1989] developed a control volume model to estimate the amount of water vapor transported by barometric pumping. *Martinez and Nilson* [1999] presented a theory for the migration of water vapor at depth in a fractured medium induced by barometric pumping.

2.5.7. Methane Transport

[44] A changing atmospheric pressure exerts a pumping effect on the soil gas, drawing gas out from the ground during periods of decreasing pressure and forcing atmospheric air into the ground during periods of increasing pressure [*Pinault and Baubron*, 1997; *Gebert and Groengroeft*, 2006]. Barometric pumping has been found to have a significant influence on trace gases movement through any highly permeable medium [*Klusman and Jaacks*, 1987; *Massman et al*., 1995]. *Christophersen et al*. [2001] observed that during a drop in atmospheric pressure the landfill gas (CH_4 and CO_2) fluxes changed dramatically within a very short time. They concluded that increasing the atmospheric pressure decreases the landfill gas fluxes due to a decreasing pressure gradient between the landfill and the atmosphere and the landfill gas fluxes are very dependent on atmospheric pressure changes. On the other hand, decreasing atmospheric pressure was found to increase the landfill gas emissions [*Young*, 1992; *Nastev et al*., 2001].

[45] The increase in the atmospheric concentration of methane (CH_4) makes it become the second most important greenhouse gas after CO_2 [*Herbst et al*., 2011]. Many researchers found that a drop in atmospheric pressure leads to an increase in CH_4 emissions [*Mattson and Likens*, 1990; *Christophersen et al*., 2001; *Gebert and Groengroeft*, 2006; *Tokida et al*., 2005, 2007; *Sachs et al*., 2008]. On the other hand, CH_4 fluxes were observed to decrease markedly during calm high-pressure periods [*Mattson and Likens*, 1990; *Sachs et al*., 2008]. Negative correlation between CH_4 flux and changes in atmospheric pressure [*Börjesson and Svensson*, 1997; *Christophersen et al*., 2001; *Gebert and Groengroeft*, 2006] and the absolute value of atmospheric pressure [*Czepiel et al*., 1996; *Christophersen et al*., 2001; *Czepiel et al*., 2003] was obtained.

In addition, researchers also found that episodic CH_4 emissions are associated with drops in atmospheric pressure [*Windsor et al*., 1992; *Shurpali et al*., 1993; *Glaser et al*., 2004; *Tokida et al*., 2007].

[46] On the contrary, some researchers found that there is no effect of atmospheric pressure changes on CH_4 emissions. *Börjesson and Svensson* [1997] obtained no correlation between CH_4 emissions and atmospheric pressure or changes in atmospheric pressure when data were taken monthly. Furthermore, peak CH_4 fluxes were also found to be not associated with variations in atmospheric pressure [*Windsor et al*., 1992; *Herbst et al*., 2011]. In order to accurately determine the effects of atmospheric pressure changes on CH_4 emissions, continuous measurements with very short time intervals are required [*Christophersen et al*., 2001; *Tokida et al*., 2007].

2.5.8. Transport of Other Trace Gases

[47] Fluctuations in atmospheric pressure may also significantly affect the emissions of other trace gases. *Baldocchi and Meyers* [1991] stated that atmospheric pressure fluctuations may play a significant role on the emissions of trace gases from forest soils, such as N_2O, NO, and H_2S. *Meyers and Baldocchi* [1993] found that turbulence in the lower canopy of a deciduous forest is in part induced by low-frequency pressure perturbations, and at least 50% of air-surface exchange at the forest floor is dominated by the turbulent events. However, *Hinkle* [1994] concluded from observation data that there is no impact of atmospheric pressure variations on He, O_2, and N_2 concentrations.

[48] The release of soil gas at the soil surface is a combination of molecular diffusion and advection [*Thorstenson and Pollock*, 1989a, 1989b; *Massman et al*., 1995, 1997; *Etiope and Martinelli*, 2002]. *Young* [1990] developed a model to investigate the effects of variations in atmospheric pressure on the volumetric changes in landfill gas emissions. *Young* [1992] developed a model for multispecies landfill gas migration in response to fluctuations in atmospheric pressure. *Nastev et al*. [2001] developed the numerical model TOUGH2-LGM to simulate landfill gas production and migration. *Poulsen et al*. [2001] conducted numerical modeling to investigate lateral gas transport in soil adjacent to old landfill. *Poulsen and Møldrup* [2006] investigated the effects of wind-induced pressure fluctuations on landfill gas transport and emission using stochastic modeling. *Massman et al*. [1997] developed diffusion and pressure-pumping models to estimate N_2O and CH_4 fluxes through snowpack.

3. Airflow Induced by Topographic Effect

3.1. Topographically Induced Air Circulation

[49] Topographic effect can induce air circulation in unsaturated zones by thermally induced convection [*Weeks*, 1987; *Thorstenson et al*., 1989; *Sundal et al*., 2008]. The mechanism of topographic effect was explained in detail by *Weeks* [1987] which can be summarized as following. In an area of topographic relief, the column of air extending from a fractured rock outcrop on the hillside to the hillcrest will be colder, drier, and denser during cold weather than the column of air extending from the hillside outcrop through the highly permeable fractured rock and the well to the same hillcrest altitude. As a result, air will enter the outcrop and migrate upward through the fractured rock to exhaust out the well during winter. During summer, the pattern of circulation should be reversed with the well takes in air in hot weather.

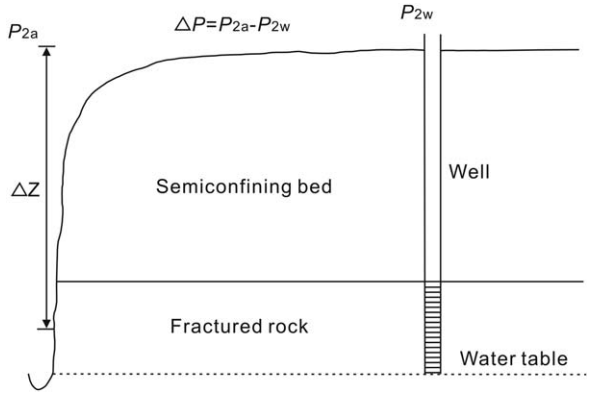

Figure 3. Schematic of the topographic effect on convective airflow (modified from *Weeks* [1987]). The quantity P_{2w} is the air pressure at the top of the well casing, P_{2a} is the atmospheric pressure at an altitude the same as the top of the well casing, ΔP is the pressure difference, and ΔZ is the difference in altitude between outcrop and the top of the well casing.

[50] *Weeks* [1987] observed substantial airflow in wells tapping highly fractured welded tuffs at the crest of Yucca Mountain, Nevada (Figure 2). The mountain forms a north-south trending ridge with a steep western scarp rising about 250 m above the Solitario Canyon floor. The east flank is a highly dissected dip slope [*Weeks*, 1987]. Two wells (UZ6 and UZ6S) were drilled through thick sections of unsaturated fractured rock at the crest of Yucca Mountain and left open. The first three zones of the formations below the well sites consist of 125 m highly fractured welded tuff, about 30 m of sparsely fractured nonwelded and bedded tuff, and about 300 m of highly fractured, moderately to densely welded tuffs (Figure 2).

[51] Because of the topographic and geologic setting of these wells, it was expected that there should be a pattern of continuous or nearly continuous air exhaust during winter. A field study indicated that this was indeed the case, with both wells exhausting air at a typical rate of about 3 m/s [*Weeks*, 1987]. This air exhalation is due plausibly to the topographic effect, in which the column of cold dry air extending from the outcrop in the valley upward to the hillcrest is heavier than the column of warm moist air extending from the outcrop through the fractured rock to the open borehole and up to the hillcrest (Figure 3). On the basis of an equation provided by *Sanford* [1982], *Weeks* [1987] estimated the potential pressure difference (ΔP in Figure 3) between the atmosphere and the top of well casing due to this topographic effect to be 0.072 kPa.

[52] According to the topographic effect, the wells should intake air nearly continuously during summer. However, observation data show that the flow direction in well UZ6S reversed repeatedly each day and the well exhausted air for substantial periods of time. *Weeks* [1987] suggested that the topographically induced air circulation may occur simultaneously with barometric pumping, which is also

pointed out by *Thorstenson et al*. [1989]. When the atmospheric pressure decline induced pressure drop from the formation to the well exceeds the topographically induced pressure difference, the reversals probably occur, and the well will begin to exhaust air [*Weeks*, 1987].

[53] Such air circulation occurs even in the absence of open boreholes. *Sundal et al*. [2008] illustrated the topographically induced air circulation in an ice-marginal deposit. In winter, the soil air flows toward the area of highest elevation, since the soil air temperature is higher than the atmospheric air temperature. In summer, soil air flows toward the area of lowest elevation because the soil air temperature is lower than the atmospheric temperature.

[54] Apart from the thermal-topographic effect and barometric pumping, wind effect is found to be another mechanism that results in air discharge from a well [*Woodcock and Friedman*, 1979; *Woodcock*, 1987; *Weeks*, 1991]. *Thorstenson et al*. [1989] noted that the high-velocity nearly continuous air exhaust at borehole UZ6S observed in winter is too large to be explained by the first two mechanisms. *Weeks* [1991] pointed out that a portion of this excess airflow is due to the wind effect. The wind generates lift and drag effects, which in turn cause pressure differences [*Weeks*, 1991]. Such pressure differences will contribute to the air discharge from a well. *Woodcock and Friedman* [1979] concluded that winds obviously altered the flow of air in a drill hole at the summit cinder cone on Mauna Kea volcano, Hawaii. *Woodcock* [1987] also concluded that wind speed has a marked effect on the airflow from the Mauna Kea summit cones. During 23 h of fresh to strong winds in December 1975, *Woodcock* [1987] observed rapidly and continuously airflow out of a drill hole in the top of the summit cone of Mauna Kea volcano. In addition, it is observed that the ventilation rates increase with wind speed [*Woodcock*, 1987]. On the basis of regression analysis, *Weeks* [1991] estimated that the wind effects accounted for about 30% of the total flow at Yucca Mountain. The influence of the wind direction was also included in his analysis. Wind has also been found to affect the airflow in snow, which is known as wind pumping [e.g., *Clarke et al*., 1987; *Colbeck*, 1989; *Cunningham and Waddington*, 1993]. Analytical solutions were derived to describe the airflow in snow [*Clarke et al*., 1987; *Colbeck*, 1989; *Clarke and Waddington*, 1991; *Cunningham and Waddington*, 1993; *Waddington et al*., 1996; *Colbeck*, 1997]. In addition to the analytical studies, numerical modeling [*Albert*, 1996; *Albert et al*., 2002] and field work [*Schwander et al*., 1993; *Albert and Shultz*, 2002] have also been done to investigate the wind pumping phenomenon.

3.2. Applications of Induced Airflow

3.2.1. Unsaturated Zone Gas Transport

[55] The topographic effect can induce gas circulation in the unsaturated zone and transport of water vapor and other gases [*Woodcock and Friedman*, 1979; *Kipp*, 1987; *Weeks*, 1987; *Woodcock*, 1987; *Thorstenson et al*., 1989; *McGee et al*., 2000; *Sundal et al*., 2008] from unsaturated zone to atmosphere. *Weeks* [1987] estimated that the two wells UZ6 and UZ6S drilled at the crest of Yucca Mountain discharged about 560 L/d and 125 L/d of water, respectively. On the basis of numerical modeling, *Kipp* [1987] estimated the net water vapor transported out from the simulation region was equivalent to 0.042 mm/yr precipitation. *Kipp* [1987] attributed this very small value to model simplification and parameter uncertainty. Topographically induced water vapor transport is also potentially important in drying the upper part of unsaturated zone rocks to a lower water content than that obtained by gravity drainage alone [*Weeks*, 1987]. Such drying would reduce precipitation infiltration and thus reduce the hazard of leaching radionuclides in a high-level radioactive waste repository [*Weeks*, 1987; *Kipp*, 1987]. The convective air circulation would also accelerate the movement of gaseous radionuclides from the repository to the atmosphere [*Weeks*, 1987]. *Thorstenson et al*. [1989] found that substantial quantities of water vapor and CO_2 were discharged from UZ6S. Topographically induced convection has also been found to affect the seasonal variations in soil radon concentrations [*Sundal et al*., 2008]. The effects of orographic wind on the transport of CO_2 were investigated by *McGee et al*. [2000]. Furthermore, the air exchange between the snow and the atmosphere induced by wind can significantly affect the heat budget and the transport of water vapor and chemical species [e.g., *Gjessing*, 1977; *Albert and McGilvary*, 1992; *Cunningham and Waddington*, 1993; *Albert*, 1996; *Waddington et al*., 1996; *Albert et al*., 2002; *Dominé and Shepson*, 2002; *Lehning et al*., 2002].

3.2.2. Mine Natural Ventilation

[56] Although topographically induced gas circulation through wells in unsaturated zone has not been widely noted, the phenomenon has been recognized and exploited for natural ventilation in mines since at least the 16th century [*Hoover and Hoover*, 1912]. Natural ventilation is the term used to describe airflow resulting from pressure difference caused by thermal energy due to temperature differences [*Sanford*, 1982; *Wala et al*., 2002; *Dalgic and Karakus*, 2004]. The pressure difference which causes the airflow is known as natural ventilation pressure (NVP) [*Wala et al*., 2002; *Dalgic and Karakus*, 2004]. It depends upon the difference in elevation of the surface and the mine workings and the difference in air temperature inside and outside the mine [*Sanford*, 1982; *Hartman et al*., 1997; *Dalgic and Karakus*, 2004]. The magnitude of NVP is usually less than 0.124 kPa and seldom exceeds 0.746 kPa [*Sanford*, 1982]. The quantity of airflow varies with the mine resistance but ordinarily is a few cubic meters per second and is less than 47.2 m^3/s [*Sanford*, 1982; *Dalgic and Karakus*, 2004]. In deep underground mines, possible values of NVP according to mine depth are given by *Wala et al*. [2002].

[57] Surface temperature changes between summer and winter. However, temperatures in mines vary little. Typically, surface temperatures in summer are higher than those in the mine, and vice versa in winter. In order to determine the direction of airflow resulting from natural ventilation in simple circuits, *Sanford* [1982] suggested the following procedures: (1) Visualize columns of air of equal height between two horizontal datum lines in order to compare the gas pressure difference. The columns should extend between the highest and lowest points in the mine. (2) Consider surface temperatures to be colder than those in the mine in winter, and vice versa in summer. (3) The colder, heavier column of air will displace the warmer, lighter column. (4) The direction of airflow will be from the heavier column toward the lighter one. For example, consider the

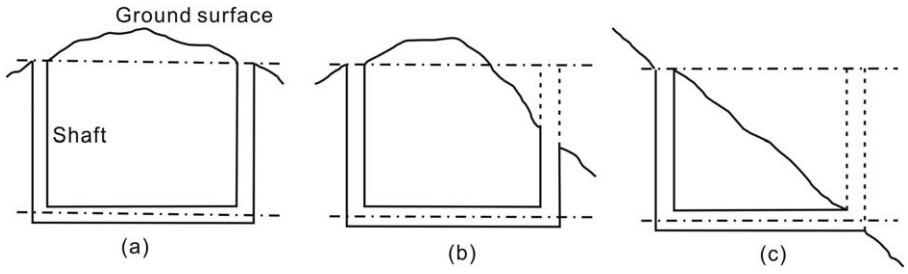

Figure 4. Determination of the direction of airflow in simple natural ventilation systems (modified from *Sanford* [1982]).

three simple mines shown in Figure 4, each showing two shafts and the connecting airway between them. The flow directions determined from the above procedures are listed in Table 1. It should be noted that in Figure 4a, the difference in elevation between the two openings at the surface is small, and flow may have to be induced. However, once the flow is induced, it will continue as long as a favorable temperature difference exists between the mine and the ground surface [*Sanford*, 1982; *Hartman et al*., 1997].

[58] Natural ventilation pressure changes frequently in magnitude and directions. If the temperature difference decreases to zero, airflow ceases. The direction of airflow will also reverse if the surface temperature changes from being less than the mine temperature to above the mine temperature. This alternation of flow direction can occur not only seasonally but also even daily. Hence, the direction of airflow in mines induced by natural ventilation is seldom constant, particularly in shallow mines [*Sanford*, 1982; *Hartman et al*., 1997; *Dalgic and Karakus*, 2004]. Natural ventilation is usually strongest in winter and weakest in summer [*Sanford*, 1982; *Hartman et al*., 1997]. *Dalgic and Karakus* [2004] found that the quantity of air obtained in the Guleman Kef chromium mine by natural ventilation is neither sufficient nor uniform. Although the ventilation in existing mines is nearly always mechanical, it is often supplemented by natural ventilation, at least in part [*Sanford*, 1982; *Wala et al*., 2002].

3.2.3. Tunnel Natural Ventilation

[59] Natural ventilation is one of the several ways to ventilate a tunnel [*Singh*, 1982; *Chang and Rudy*, 1990; *Sambolek*, 2004]. Forced ventilation without any natural ventilation at all is very seldom [*Sambolek*, 2004]. Vehicular tunnels with little or no elevation difference between the two sides often have some natural ventilation [*Sanford*, 1982]. This is due to the temperature difference on the surface at the two portals, which is caused by weather conditions on one and on the other side of the tunnel [*Sanford*, 1982; *Sambolek*, 2004]. Generally, the length of the tunnel determines the type of ventilation system employed [*Chang and Rudy*, 1990]. Natural ventilation is usually used in tunnels with relatively short length, i.e., under 300 m long [*Singh*, 1982; *Chang and Rudy*, 1990; *O'Dwyer*, 2010]. In addition to vehicular tunnels, researchers also investigated natural ventilation in dead-end tunnels [*Richon et al*., 2004; *Perrier et al*., 2007].

4. Airflow Induced by Water Table Fluctuations

4.1. Fluctuations of Water Table

[60] Fluctuations of water table can be induced by many natural factors, such as evapotranspiration, meteorological phenomena (atmospheric pressure fluctuations, rainfall recharge, wind, and frost), and tides (sea tides and earth tides) [*Freeze and Cherry*, 1979; *Todd*, 1980]. Based on the time scale of the fluctuations, the fluctuations of water table can be divided into secular fluctuations, seasonal fluctuations, and short-term fluctuations [*Todd*, 1980].

[61] In investigating the airflow induced by water table fluctuations, only the short-term fluctuations need be considered. On the basis of field measurements from eight sampling periods over 6 years at Picatinny Arsenal, New Jersey, *Tillman and Smith* [2005] found that water table changes no more than a few centimeters during several-day periods. Hence, in noncoastal areas, airflow induced by the water table changes can be ignored. However, in tidal influenced coastal areas, the fluctuations of water table are usually of high frequency and significant airflow may be induced by the high-frequency fluctuation of the water table [*Parker*, 2003].

[62] Tides are the periodic rise and fall of sea level due to the gravitational attraction of the sun and the moon acting on ocean waters. Based on the number of high tides and low tides per day and their relative heights, tides can be divided into three general types: diurnal tides, semidiurnal tides, and mixed tides [e.g., *Marmer*, 1926; *Gross*, 1990; *Segar*, 1998]. Diurnal tides (or daily tides) have only one high tide and one low tide in each tidal day. Semidiurnal tides (or semidaily tides) have two high and two low tides of approximately equal heights each tidal day. Mixed tides also have two high tides and two low tides each day, but the heights of the two high tides (and/or of the two low tides) are different. Among these types of tides, mixed tides are the most common [*Segar*, 1998].

[63] Tidal fluctuation of the sea surface is on the magnitude of several meters each day [e.g., *Marmer*, 1926; *Gross*, 1990; *Segar*, 1998; *Reddy*, 2001]. *Nielsen* [1990] observed that the tide on Barrenjoey Beach north of Sydney, Australia, was almost sinusoidal, semidiurnal with amplitude of 0.516 m during 18–19 April 1989. *Jiao and Li* [2004] presented observations of the sea tide near a coastal reclaimed area in Hong Kong and found that the amplitude

Table 1. Flow Directions for the Simple Natural Ventilation Systems (From *Sanford* [1982])

	Figure 4a	Figure 4b	Figure 4c
Need to induce	Yes	No	No
Direction, winter	Either	Right to left	Right to left
Direction, summer	None	Left to right	Left to right

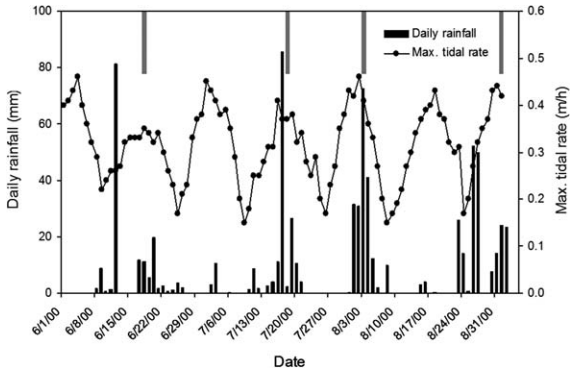

Figure 5. Daily rainfall and tidal rate in the Hong Kong International Airport. The days with heave damage are marked in gray bars.

of the tide is 1.25 m during the 72 h period from 7 to 9 February 2001. *Li et al*. [2007] observed that the amplitude of the diurnal fluctuation of the sea tide in a coastal area in Shandong, China, is 1.1 m during the 48 h period from 3 to 4 August 1998.

4.2. Air Pressure Fluctuations in Coastal Unsaturated Zones

[64] Subsurface airflow caused by water table fluctuations induces effects similar to that of the airflow driven by barometric pressure fluctuations [*Camp Dresser and McKee*, 1986], although typically of lesser magnitude unless the water table fluctuations are of high frequency (e.g., in tidal influenced coastal unsaturated zones) [*Parker*, 2003]. Understanding subsurface airflow in coastal unsaturated zones induced by sea tides is of both theoretical and practical significance for coastal environmental and engineering problems [*Jiao and Li*, 2004]. Although tide-induced groundwater flow has been extensively studied [e.g., *Jacob*, 1950; *Ferris et al*., 1962; *Carr*, 1971; *Nielsen*, 1990; *Sun*, 1997; *Jiao and Tang*, 1999; *Li and Barry*, 2000; *Li and Jiao*, 2001; *Li et al*., 2002, 2007; *Guo et al*., 2010; *Bobo et al*., 2012; *Huang et al*., 2012], tide-induced airflow in coastal vadose zones has not been well addressed.

[65] Subsurface air pressure in coastal unsaturated zones fluctuates in response to sea tides, as does the water table in the aquifers. When the water table rises, the air pressure in the unsaturated zone increases, this higher pressure will propagate to the ground surface and the air is pushed to escape from the ground surface, thus the ground surface exhales. When the water table falls, the process is reversed and the surface air is introduced into the subsurface, thus the ground surface inhales [*Jiao and Li*, 2004]. In most of the cases, such a breathing process is not obvious and may be undetectable by human. However, if the superficial soil has low permeability, or heavy rainfall seals off the pores of the soil, the air exchange between the soil and the atmosphere is blocked or reduced so that very high and low pressures can be induced, respectively, when water table rises and falls. For example, fluctuations of subsurface air pressure ranging between −1 and 2 kPa were observed in coastal areas in Hong Kong [*Jiao and Li*, 2004].

[66] Large-scale coastal land reclamation has been conducted in many coastal areas because more and more people choose to work and live in these areas. Many important structures such as sea ports, container terminals, and airports are built on areas reclaimed from the sea. A common feature of these structures is the areally extended asphalt or concrete ground surface. The air permeability of this surface is low and can be even lower under heavy rains, when rainwater seals off the pores of the materials. To support heavy vehicles, especially the airplanes, the fill materials under this surface are usually coarse rock fragments or gravels which have many voids for air storage. In such well-capped areas, the subsurface air pressure generated when the sea tide rises rapidly during heavy rainfall periods can be so high that it causes surface heave. For example, dome-shaped heave features have been observed in areally extensive asphalt pavement in Hong Kong International Airport, which is an artificial reclaimed island [*Jiao and Li*, 2004; *Leung et al*., 2007]. At some locations, the dome-shaped heaves were observed to be with a height of up to 0.4 m and a diameter up to approximately 10 m [*Leung et al*., 2007]. The concrete surface heaved four times in the summer of 2000 (Figure 5). Figure 5 also shows the rainfall and tide rate in the summer. Heaves occurred when both the tide rate and rainfall intensity are great (Table 2). On 12 June, rainfall was heavy but tidal rate was insignificant. Around the days of 1 July and 18 August, the tide rate was high but the rainfall was low. There was no heave damage in these days.

[67] To understand the abnormally high air pressure under the asphalt pavements in the Hong Kong International Airport, *Jiao and Li* [2004] used an isothermal, two-dimensional cross-section model to investigate the air-water two-phase flow induced by the sea tide and rainfall infiltration. TOUGH2 [*Pruess et al*., 1999] was used to obtain numerical solutions of the model. Air permeability of the asphalt was determined by the methods developed by *Li et al*. [2004] and *Li et al*. [2011b]. The model was first calibrated against the observed subsurface air pressure under no rain conditions and then used to demonstrate that abnormally high and low air pressures could be generated by a combination of geological structure, quickly fluctuating tidal level, and heavy rainfall. The simulated maximum and minimum air pressure under no rain conditions at a observation point were 1.64 and −0.56 kPa, respectively. Under rain conditions, the maximum air pressure could be 2–3 times higher than under no rain conditions and the minimum air pressure could be 5–9 times lower than under no rain conditions.

[68] Figure 6 presents the observed air pressure at the observation point beneath an extensive pavement in the Hong Kong International Airport, together with tidal level and barometric pressure during 7–9 February 2001 [*Jiao and Li*, 2004]. It can be seen from Figure 6a that the observed

Table 2. Tidal Rate and Rainfall in the Days of 2000 With Heave Damage

Date	Daily Rainfall (mm)	Maximum Tide Rate (m/h)
18 June	11.2	0.35
18 July	2.4	0.37
3 August	72.5	0.41
1 September	23.9	0.42

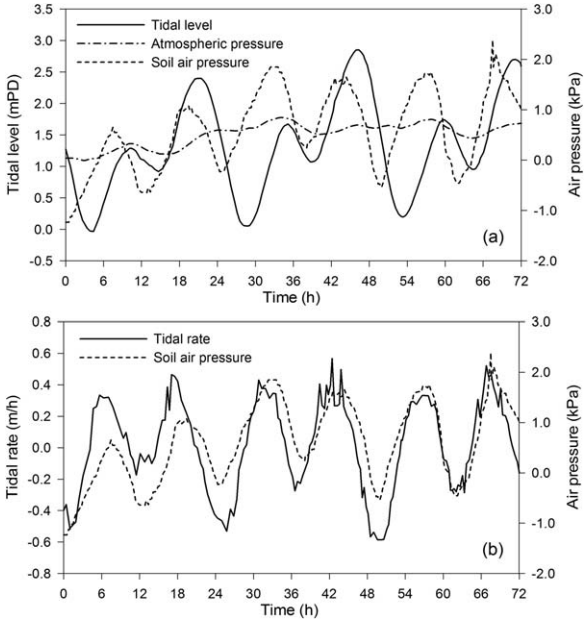

Figure 6. (a) Observed sea tide, subsurface air pressure, and barometric pressure during the 72 h period from 7 to 9 February 2001 and (b) comparison of observed air pressure and tidal rate (modified from *Jiao and Li* [2004]).

subsurface air pressure fluctuation is much greater than the atmospheric pressure fluctuation, so the latter cannot be the direct driving force of the former. The simulation results show that the subsurface air pressure is approximately proportional to the rate of tidal rise and fall [*Jiao and Li*, 2004], as shown in Figure 6b. The times when the air pressure reaches its peaks are in line with that of the rate of tidal rise and fall. This suggests that the maximum air pressure is determined by the maximum tidal rising rate, rather than the amplitude of the tide. If the tidal level rises slowly, a high tidal level does not necessarily lead to a high air pressure. However, a sudden rise of the tidal level results in high air pressure, although the amplitude of the tidal level rise may not be great. This explains why the tide with small and large peaks can induce similar air pressure peaks (Figure 6a).

[69] The simulated air pressure and airflow velocity distributions under no rain conditions are shown in Figure 7 [*Jiao and Li*, 2004]. Negative air pressure is generated and the ground inhales when the water table falls. The falling of the water table creates extra pore spaces; hence, air flows from the atmosphere into the unsaturated zone to fill the pores. Columns of low air pressure are formed below the pavement surfaces. High air pressure is generated and the ground exhales when the water table rises. Figure 7b clearly shows that the rising water table compresses the air and forces the air to exhale through the ground surface, as clearly indicated by the airflow velocity distributions. In this case, columns of high air pressure are formed below the pavement surfaces.

[70] *Guo and Jiao* [2008] presented numerical simulations of air-water two-phase flow induced by sea tides in a general coastal two-layered unsaturated zone. The model consists of a highly permeable lower layer and a less permeable upper layer. *Guo and Jiao* [2008] used TOUGH2 [*Pruess et al*., 1999] to obtain numerical solutions of the model for different cases. A single-component sinusoidal, diurnal tide was used as the tidal level variation at the coastline. Simulation results show that when the permeability of the lower layer was fixed at 10^{-11} m^2, and the permeability of the upper layer was set to be 1.77×10^{-14}, 1.14×10^{-13}, and 1.12×10^{-12} m^2, the corresponding amplitudes of the air pressure fluctuation in the unsaturated zone of the lower layer were 2.33, 1.64, and 0.33 kPa, respectively. When the permeability of the upper layer is about 2 orders of magnitude lower than that of the lower layer, the system can be called an air-confined system [*Guo and Jiao*, 2008, 2010]. The tide induced water table fluctuation may result in significant air pressure fluctuation in the unsaturated zone of the lower layer. In such an air-confined system, vertical airflow is dominant in the upper layer and horizontal airflow is dominant in the lower layer. The air flux across the soil-atmosphere interface attenuates landward gradually. This attenuation becomes faster when the permeability of the upper layer increases. Otherwise, the system is air-unconfined and the fluctuation of air pressure can be ignored [*Guo and Jiao*, 2008, 2010].

[71] When the sea level falls, vacuum can be generated in the unsaturated zone and the fine materials such as silt and clay particles in the unsaturated zone can be soaked away by the generated vacuum. When this process has undergone for a long time, underground caves or holes can be generated. It is believed that some coastal subsidence and caves are probably caused by this process.

4.3. Single-Phase Airflow Model

[72] Analytical studies were also conducted to investigate the airflow induced by sea tides in coastal layered unsaturated zones. In these analytical studies, the original nonlinear model of air-water two-phase flow was simplified

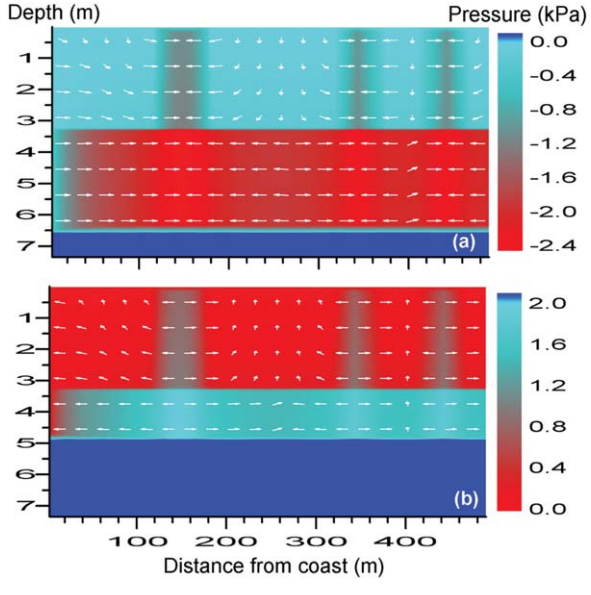

Figure 7. Simulated subsurface air pressure (color) and airflow velocity (arrows) distributions under no rain conditions when (a) water table falls and (b) rises (from *Jiao and Li* [2004]).

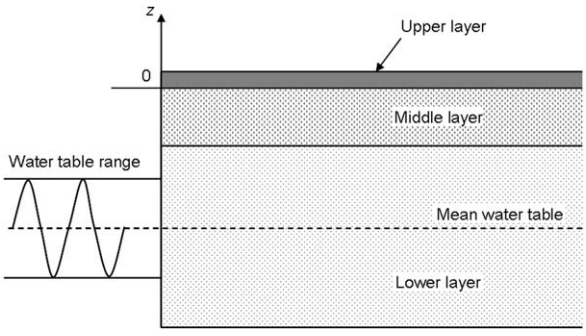

Figure 8. Schematic of airflow induced by sea tide in a coastal multilayered unsaturated zone (modified from *Xia et al*. [2011]).

into a linear single-phase airflow model. The flow was also assumed to be one-dimensional in the vertical direction. The atmospheric pressure was assumed to be a constant [*Li and Jiao*, 2005; *Xia et al*., 2011]. *Li and Jiao* [2005] stated that the fluctuations of atmospheric pressure can easily be considered by subtracting the atmospheric pressure fluctuation data from the subsurface air pressure without loss of much accuracy. The density difference in salt water and freshwater was also ignored. Additional assumptions and approximations are given by a number of researchers [*Li and Jiao*, 2005; *Li et al*., 2011a; *Xia et al*., 2011; *Li et al*., 2012b].

[73] The governing equation was chosen as equation (4) for the single-phase airflow model. The upper boundary was set to be the constant atmospheric pressure at the ground surface. The lower boundary was controlled by the tide-induced local fluctuation of the hydraulic head of the unconfined aquifer, which was assumed to be synchronous with tidal fluctuations and is usually expressed as [e.g., *Nielsen*, 1990]

$$H(t) = -D + \sum_{j=1}^{N} A_j \cos\left(\omega_j t + \varphi_j\right) \tag{7}$$

where D is the distance from the ground surface (datum) to the mean water table, N is the number of sinusoidal components of the tide-induced local head fluctuation, A_j, ω_j, and φ_j are the amplitude, frequency, and phase shift of the jth component of the local head fluctuation, respectively.

[74] The first analytical solution derived to investigate the vertical airflow driven by fluctuating water table within the lower layer of a coastal two-layered system is given by *Li and Jiao* [2005]. The reasonability of the derived analytical solution was examined by numerical solutions of the original nonlinear model using TOUGH2 [*Pruess et al*., 1999]. Under certain conditions, similar conclusions were obtained using the analytical solution to that of the numerical simulations by *Jiao and Li* [2004]. *Li et al*. [2011a] expanded *Li and Jiao*'s [2005] model to consider the fluctuations of atmospheric pressure. A new semianalytical transient solution was developed to the airflow model which can deal with an initial boundary value problem. The results reveal that the impact of atmospheric pressure fluctuations on subsurface air pressure depends on the air resistance in the less permeable upper layer and the air-filled porosity difference in the two layers. The results also show that the influence of atmospheric pressure fluctuations on water table is insignificant. *Song et al*. [2013] improved on the semianalytical solution of *Li et al*. [2011a] and derived an explicit analytical solution. *Xia et al*. [2011] derived an analytical solution to interpret the subsurface air pressure fluctuation induced by sea tides in a coastal three-layered unsaturated zone (Figure 8). If the upper layer is very permeable or disappears, the solution becomes that of *Li and Jiao* [2005]. Calculations show that the low-permeability upper layer played an important role in generating abnormally high air pressure fluctuations below it.

4.4. Applications of Induced Airflow

4.4.1. Air Permeability Estimation

[75] The analytical solutions can be used to estimate the air permeability of the upper layer. On the basis of the fitting to the observed tidal level fluctuations and the amplitudes of subsurface air pressure fluctuation, *Li and Jiao* [2005] estimated that the value range of the air permeability of the marine sand fill at Hong Kong International Airport is between 1.2×10^{-12} and 2.0×10^{-12} m^2. *Li et al*. [2012a] developed a time series Fourier analysis method to determine the air permeability of the less permeable upper layer based on the model developed by *Li and Jiao* [2005]. The method used the amplitude attenuations of subsurface air pressure to calculate the air permeability. The method was applied to determine the air permeability of the marine sand fill at Hong Kong International Airport. Results show that the determined air permeability ranges from 6.9×10^{-13} to 5.9×10^{-12} m^2. However, the air permeability value calculated based on the amplitude attenuations of diurnal and semidiurnal components in the Fourier series is 1.2×10^{-12} m^2.

4.4.2. Other Applications

[76] Subsurface air pressure fluctuations induced by sea tides may be used as an alternative to clean coastal aquifers contaminated by VOCs [*Jiao and Li*, 2004]. The induced air circulation may cause the vertical diffusivity of contaminants to be orders of magnitude larger than that by molecular diffusion alone [*Jiao and Li*, 2004]. *Pierdinock and Fedder* [1997] presented a case study on the selection, design, and installation of a bioslurping remediation system in a tidally controlled geological formation. Tide-induced airflow in coastal vadose zones may also have some ecological effects on coastal plants and organisms because the gas circulation will enhance the transport of oxygen and nutrients in the subsurface soil [*Jiao and Li*, 2004; *Ursino et al*., 2004; *Li et al*., 2005]. On the basis of the work of *Ursino et al*. [2004], *Li et al*. [2005] investigated the tidal effects on aeration conditions for plant root respiration in a tidal marsh using an air-water two-phase flow numerical model. Simulations were conducted to examine the link between the air movement and the aeration condition in the marsh soil.

5. Airflow Induced by Infiltration

5.1. Impact of Airflow on Infiltration

[77] The infiltration process involves water inflow and air outflow. When water infiltrates, infiltrated water

displaces soil air, and the air is expelled from the soil through the soil surface. If the soil air ahead of the wetting front can freely escape, the impact of air on infiltration can be ignored, and the classical unsaturated flow theory seems to be adequate for modeling the infiltration process [*Touma and Vauclin*, 1986]. However, when there is a shallow water table, an impermeable layer, or a lateral obstruction, the soil air may become entrapped and cannot escape freely [e.g., *Slater and Byers*, 1931; *Adrian and Franzini*, 1966; *Norum and Luthin*, 1968; *Touma and Vauclin*, 1986; *Sabeh*, 2004; *Lukyanets*, 2010]. The entrapped air is compressed as the infiltration process continues. The air compression and subsequent air counterflow may reduce infiltration rates and result in potential practical problems of excess runoff and erosion [e.g., *Free and Palmer*, 1941; *Horton*, 1941; *Adrian and Franzini*, 1966; *Dixon and Linden*, 1972; *Jarrett and Fritton*, 1978; *Suhr et al*., 1984; *Grismer et al*., 1994; *Wang et al*., 1998; *Wangemann et al*., 2000]. Air compression in front of the wetting front may also cause wetting front instability and preferential flow or fingered flow [e.g., *Saffman and Taylor*, 1958; *Peck*, 1965b; *Raats*, 1973; *Philip*, 1975; *White et al*., 1977; *Vauclin*, 1989; *Wang et al*., 1998]. The induced airflow also has important implication for groundwater recharge.

[78] The magnitude of air pressure buildup ahead of the wetting front is generally on the order of tens of centimeters of water column height, as observed both in laboratory column tests [e.g., *Peck*, 1965a, 1965b; *Vachaud et al*., 1973, 1974; *Touma and Vauclin*, 1986; *Latifi et al*., 1994; *Grismer et al*., 1994; *Wang et al*., 1998] and in the field [*Dixon and Linden*, 1972; *Linden and Dixon*, 1973; *Linden et al*., 1977]. An example of air pressure buildup ahead of the wetting front during air compression and counterflow in a soil column bounded by a shallow water table is shown in Figure 9 [*McWhorter*, 1971]. It can be seen that the air pressure first increased to a maximum value, then decreased quickly when air breakthrough occurred at the soil surface, and again increased slowly. The time evolutions of air pressures show similar trends to Figure 9 if air breakthrough occurred at the soil surface [e.g., *McWhorter*, 1971; *Dixon and Linden*, 1972; *Linden and Dixon*, 1973; *Linden et al*., 1977; *Touma and Vauclin*, 1986; *Grismer et al*., 1994]. More complicated air pressure patterns were also observed [e.g., *Peck*, 1965b; *Grismer et al*., 1994; *Latifi et al*., 1994; *Wang et al*., 1998]. In some cases, the air pressures increased steadily without significant decrease [e.g., *Peck*, 1965b; *McWhorter*, 1971; *Vachaud et al*., 1974; *Linden et al*., 1977; *Grismer et al*., 1994; *Wang et al*., 1998; *Lukyanets*, 2010].

[79] In horizontal columns of slate dust and sand, *Peck* [1965a] observed that the maximum air pressure buildup for the slate dust is about 55 cm of water column height and for the sand is about 12 cm of water column height, respectively. In vertical columns of the same materials, *Peck* [1965b] observed that the pore air pressures in bounded vertical columns of slated dust and sand increased to about 50 cm and over 40 cm of water, respectively. In a stratified vertical column of sand with rain intensity of 3 cm/h, *Vachaud et al*. [1973] found that the soil air pressure increased to about 50 cm of water larger than the atmospheric pressure. *Grismer et al*. [1994] found that the maximum air pressure buildup ranges from 17 to 50 cm of water in infiltration into soil columns bounded by shallow water tables. *Latifi et al*. [1994] investigated infiltration in vertical closed columns of homogeneous soil and vertical columns of two-layered soil with a finer grained soil being placed on top. The results showed that air pressure buildup was more pronounced in the two-layered columns than columns of homogeneous soil. The maximum air pressure buildup in the two-layered column is 60 cm of water column height, while the maximum air pressure buildup in the homogeneous column is 30 cm of water column height. In a bounded dry sand column, *Wang et al*. [1998] found that the air pressures below the wetting front at different depths increased uniformly to over 40 cm of water.

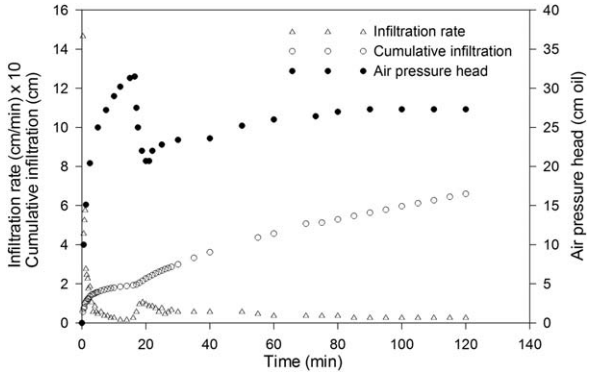

Figure 9. Infiltration in a vertical bounded column of Poudre sand of 185 cm equivalent length (modified from *McWhorter* [1971]).

[80] Even in unbounded soil systems, significant air pressure buildup ahead of the wetting front was observed by a number of researchers [*Wilson and Luthin*, 1963; *McWhorter*, 1971; *Collis-George and Bond*, 1981]. In a horizontal 31 cm column of Columbia silt loam, *Wilson and Luthin* [1963] observed that during horizontal absorption the soil air pressure reached a maximum of at least 11 cm of water a short time after the initiation of infiltration. *Bond and Collis-George* [1981] conducted several infiltration experiments in a vertical 120 cm column of fine sand with the bottom of the column open to the atmosphere. During the infiltration experiments, air is free to escape from the base of the column. *Collis-George and Bond* [1981] presented that pore air pressure in the column rose quickly to a maximum value soon after infiltration commenced and then gradually decreased. The maximum values reached at every depth almost simultaneously at 100 s after infiltration started. The maximum air pressure at 5 cm under the upper surface of the column is about 12 cm. The results were similar to that described by *Wilson and Luthin* [1963]. *McWhorter* [1971] found that the maximum air pressure buildup is about 10 cm of a light hydrocarbon oil (referred to "oil" hereafter) in a vertical 50.8 cm column of Poudre sand in which air was allowed to escape freely from the bottom of the column.

[81] Researchers also noted that the length of column has a marked effect on the air pressure buildup in laboratory column infiltration experiments [*Peck*, 1965b; *McWhorter*, 1971]. The air pressure buildup is more significant in longer columns, due to the increased resistance to flow

[*McWhorter*, 1971]. In vertical bounded columns of sand, *Peck* [1965b] observed that the maximum pore air pressures increased from about 15 cm of water to over 40 cm of water when the column lengths increased from 113 cm to 490 cm. In vertical columns of Poudre sand in which air was allowed to escape freely from the bottom of the column, *McWhorter* [1971] found that the maximum air pressure buildup is increased from slightly over 7 cm of oil for a 25.4 cm column to about 10 cm of oil for a 50.8 cm column. However, for vertical bounded columns of slate dust, *Peck* [1965b] found that the air pressure buildup decreased with increased length of the column.

[82] The air compression ahead of the wetting front and air counterflow can significantly reduce the infiltration of water into the soil, as shown by both field tests [*Bianchi and Haskell*, 1966; *Dixon and Linden*, 1972; *Linden and Dixon*, 1973, 1976; *Linden et al*., 1977; *Starr et al*., 1978; *Hammecker et al*., 2003] and laboratory column infiltration experiments [*Powers*, 1934; *Lewis and Powers*, 1939; *Free and Palmer*, 1941; *Horton*, 1941; *Wilson and Luthin*, 1963; *Peck*, 1965a, 1965b; *Adrian and Franzini*, 1966; *McWhorter*, 1971; *Vachaud et al*., 1973, 1974; *Jarrett and Fritton*, 1978; *Touma and Vauclin*, 1986; *Grismer et al*., 1994; *Latifi et al*., 1994; *Wang et al*., 1998; *Culligan et al*., 2000; *Lukyanets*, 2010]. The downward moving of the wetting front is retarded by the air pressure buildup. The infiltration is reduced by decreases in both hydraulic conductivity and hydraulic gradient [*Dixon and Linden*, 1972; *Jarrett and Fritton*, 1978; *Constantz et al*., 1988; *Grismer et al*., 1994; *Wang et al*., 1998].

[83] In laboratory experiments, observations of reduced infiltration rates due to air compression and air counterflow have been made by researchers. The reduced infiltration rates in bounded columns were compared to the infiltration rates in open columns. *Powers* [1934] observed that the rate of wetting the sandy loam in a column closed at the base was about one half of that in a column open to the atmosphere at the base. *Free and Palmer* [1941] found that it took 10–100 times longer to wet columns of silica sand closed at the base than it took to wet columns of the same material open at the base. *Horton* [1941] observed a gradual building up of air pressure within the soil mass in a bounded glass jar and the infiltration capacity at the end of the experiment was about half of that in the experiment with provision for free escape of soil air. *Adrian and Franzini* [1966] observed the infiltration rate in vertical closed column dropped essentially to zero within about 20 min. *Jarrett and Fritton* [1978] found that at 10 min after the start of the infiltration tests in the plastic container with air trapped, the average infiltration rates were reduced by 45% when the soil air was not free to escape to the atmosphere. In a bounded vertical column of alluvional coarse sand, *Touma and Vauclin* [1986] found that the infiltration is drastically reduced (Figure 10). For instance, at $t = 0.1$ h, the infiltration rate is 6 times less than the saturated hydraulic conductivity and 10 times less than the infiltration rate when air can escape freely from lateral openings. Examples on comparison of infiltration in open and bounded columns can also be found in *Vachaud et al*. [1974].

[84] In the field, several investigators made similar observations of reduced rates of infiltration due to air compression and counterflow. Under border irrigation conditions, *Dixon and Linden* [1972] observed that the displaced air pressure built to a maximum of about 19 cm and reduced the total infiltration by about 1/3. *Linden et al*. [1977] observed that soil air pressure varies directly with surface water pressure during each border irrigation and soil air pressure created and maintained from the onset of infiltration under simulated rain reduced infiltration by about 20%. *Linden and Dixon* [1976] concluded from sets of field infiltration tests that infiltration was increasingly impeded as soil air pressure increased from 0 to 0.5 kPa, and infiltration rates during the first 3 min of wetting were decreased by an order of magnitude with 0.5 kPa of air back pressure. *Starr et al*. [1978] conducted two ponded flow experiments to study the leaching characteristics of a layered field soil, coarse sand underlying fine sandy loam, with a water table at a depth of 1.8 m. Results show that the rate of infiltration increased by nearly twofold when the trapped air between the saturated surface layer and the shallow water table was vented directly to the atmosphere.

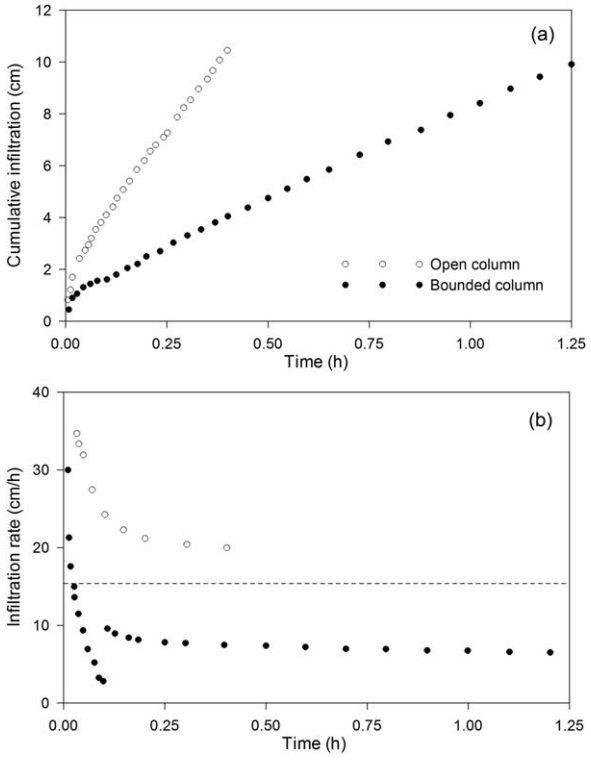

Figure 10. Evolution of (a) cumulative infiltration and (b) infiltration rate with time in the open and bounded columns during ponded infiltration (modified from *Touma and Vauclin* [1986]). The dotted line in Figure 10b is the saturated hydraulic conductivity of the coarse sand.

[85] As the infiltration process continues, the air pressure increases. When the air pressure is sufficiently high, air will escape from the soil surface and thereby causing a sharp decrease in air pressure and a significant increase in the infiltrate rate [*Free and Palmer*, 1941; *Peck*, 1965b; *McWhorter*, 1971; *Touma and Vauclin*, 1986; *Grismer et al*., 1994]. The pore air pressure required to initiate air escape from a vertical bounded column is equal to the water pressure at the bottom of the minimum depth of the saturated zone plus the air-entry pressure of the porous

material [*Peck*, 1965b; *Weeks*, 2002]. An example is shown in Figure 9 [*McWhorter*, 1971]. It can be seen that a sharp decrease in the air pressure head and a corresponding increase in the infiltration rate occurred after the air pressure head reached a maximum value of 32 cm of oil. A sharp increase in infiltration rate occurs after counterflow of air begins. It is believed that the formation of airflow channels by the escaping air is the reason for the sharp air pressure decrease observed shortly after air counterflow began, and this could also account for the increase in infiltration rates [*McWhorter*, 1971; *Grismer et al*., 1994]. *Grismer et al*. [1994] concluded from observations of bounded column infiltration experiments that infiltration rates progressively declined until the soil air pressure head exceeds the sum of the ponded water depth and the capillary driving head at the wetting front. The infiltration rate reached a minimum just prior to air breakthrough at the soil surface. The infiltration rate increased and the soil air pressure decreased when soil air broke through the soil surface. After a short transition period, during which stable airflow channels formed in the soil, the infiltration rate approached a constant value below the saturated hydraulic conductivity.

[86] While the infiltration is impeded by air compression ahead of the wetting front, air pressure lower than atmospheric pressure may increase the infiltration. Increase of infiltration rate was observed in soil columns when the soil air pressure is lower than atmospheric pressure (i.e., a vacuum exists) [*Prunty and Bell*, 2007, 2008]. In ponded infiltration into vertical columns of Hecla loamy fine sand, *Prunty and Bell* [2007] found that the time to infiltrate 50 cm^3 of water into the column shows a clear indication of shorter times at low air pressure. For falling head infiltration tests, the infiltration was also faster with vacuum conditions than the infiltration with atmospheric pressure condition. The infiltration rates at the end of the infiltration runs were 1.00 and 0.64 cm/min for vacuum conditions and atmospheric pressure conditions, respectively.

5.2. Infiltration With Airflow Model

[87] The traditional unsaturated flow theory used by researchers to model the infiltration process neglects the air effects [e.g., *Morel-Seytoux*, 1983]. However, the above analysis shows that the infiltration process may be significantly affected by airflow and the traditional unsaturated flow model using Richards' equation [*Richards*, 1931] may lead to serious error [*Morel-Seytoux and Billica*, 1985b]. Hence, the soil air pressure and its infiltration effects are not negligible when modeling infiltration processes [e.g., *Dixon and Linden*, 1972; *Linden and Dixon*, 1973; *Vachaud et al*., 1973; *Wang et al*., 1998]. Basically, there are two methods to account for the effects of air compression and air counterflow on infiltration in deriving a theoretical model. The first method is to modify the Green-Ampt model [*Green and Ampt*, 1911], and the second method is to use the air-water two-phase flow model.

5.2.1. Modified Green-Ampt Model

[88] *Green and Ampt* [1911] derived an equation that describes the infiltration of water into a vertical column of porous media under ponded conditions. The equation is based on the following assumptions: (1) the porous medium is homogeneous; (2) the hydraulic conductivity in the wetted zone is a constant, this assumption means that the water content in the wetted zone is uniform; (3) the capillary pressure at the wetting front is a constant; and (4) the wetting front is sharp. The Green-Ampt model is a piston flow model [e.g., *Bouwer*, 1969; *Whisler and Bouwer*, 1970]. The rate of water infiltration can be written as

$$i_w = K_{sw}\frac{h_0 + z_f + h_{cf}}{z_f} \tag{8}$$

where i_w is the infiltration rate, K_{sw} is the saturated hydraulic conductivity, h_0 is the water pressure head at the soil surface (depth of ponding), z_f is the vertical extent of the saturated zone (i.e., depth of the wetting front from land surface), and h_{cf} is the capillary pressure head (or soil suction) at the wetting front. A schematic diagram illustrating the meaning of equation (8) is given by *Jarrett and Fritton* [1978]. Equation (8) can be easily found in the literature [e.g., *Adrian and Franzini*, 1966; *Childs*, 1969; *Jarrett and Fritton*, 1978; *Morel-Seytoux and Khanji*, 1974; *Grismer et al*., 1994; *Wang et al*., 1997; *Hammecker et al*., 2003].

[89] The capillary pressure head h_{cf} (a positive quantity) at the wetting front is defined as the pressure head difference between air and water, which can be written as $h_{cf} = h_{af} - h_{wf}$ [e.g., *Morel-Seytoux*, 1973; *Wang et al*., 1997], where h_{wf} is the soil water pressure head at the wetting front and h_{af} is the air pressure head immediately below the wetting front. When $h_{af} = 0$, which means no air pressure buildup below the wetting front, the capillary pressure head h_{cf} is equal to $-h_{wf}$. Substituting the expression of h_{cf} into equation (8) leads to the general infiltration equation [*Adrian and Franzini*, 1966; *Grismer et al*., 1994; *Wang et al*., 1997; *Hammecker et al*., 2003]

$$i_w = K_{sw}k_{rc}\frac{h_0 + z_f + h_{cf} - h_{af}}{z_f} \tag{9}$$

where k_{rc} is the relative water hydraulic conductivity accounting for air-confining condition [*Wang et al*., 1997].

[90] There are two important parameters in the Green-Ampt model, namely, the saturated hydraulic conductivity K_{sw} and the capillary pressure h_{cf}. It has been long recognized that the hydraulic conductivity in equation (8) should not be the saturated hydraulic conductivity K_{sw} [e.g., *Bouwer*, 1969; *Whisler and Bouwer*, 1970; *Morel-Seytoux and Khanji*, 1974; *Jarrett and Fritton*, 1978; *Morel-Seytoux*, 1983]. Different values of k_{rc} were suggested by researchers. *Constantz et al*. [1988] found from a series of field and laboratory experiments that the effective hydraulic conductivity of the transmission zone remained at a level no greater than 20% of the soil's saturated hydraulic conductivity and suggested that k_{rc} ranges from 0.15 to 0.2. On the basis of limited available data, *Bouwer* [1966] generalized that $k_{rc} = 0.5$. Some researchers [*Wang et al*., 1997; *Hammecker et al*., 2003] stated that experimental data [*Vachaud et al*., 1974; *Touma et al*., 1984; *Wang et al*., 1998] also indicated that the value of k_{rc} should be about 0.5. In analysis of infiltration in layered porous media, *Ma et al*. [2010, 2011] introduced a saturation coefficient S_f ($0 < S_f < 1$) and suggested that $k_{rc} = S_f$. *Ma et al*. [2010] calculated the value of S_f as 0.8.

[91] The second parameter is the capillary pressure head h_{cf} at the wetting front. Different approaches were proposed by researchers to estimate the capillary pressure head h_{cf} [*Bouwer*, 1964; *Whisler and Bouwer*, 1970; *Mein and Larson*, 1973; *Morel-Seytoux and Khanji*, 1974; *Brakensiek*, 1977]. All the methods assumed that h_{cf} is a constant value for a certain porous medium. *Brakensiek* [1977] compared the different methods to estimate h_{cf} using data of five soils and concluded that all the methods lead to very similar h_{cf} values. *Morel-Seytoux et al*. [1996] presented an approximation of *Bouwer's* [1964] formula for *van Genuchten* [1980] soil hydraulic properties. A number of researchers [*Morel-Seytoux and Khanji*, 1974; *Grismer et al*., 1994; *Wang et al*., 1997] summarized the different approaches to estimate the value of h_{cf}.

[92] The air pressure head h_{af} ahead of wetting front can be calculated by Boyle's law [*Adrian and Franzini*, 1966; *Wang et al*., 1997; *Hammecker et al*., 2003], which can be expressed as

$$h_{af} = \frac{z_f}{L - z_f} h_{atm} \tag{10}$$

where L is the depth of airflow barrier (e.g., an air-impermeable stratum or the water table) and h_{atm} is the atmospheric pressure.

[93] Different expressions for the infiltration process considering air compression and counterflow based on the Green-Ampt model [*Green and Ampt*, 1911] were derived by researchers. One of the first models to consider the air effect was given by *Adrian and Franzini* [1966]. *Jarrett and Fritton* [1978] used soil air pressure measurements to model the infiltration process using the Green-Ampt model. *Weir and Kissling* [1992] derived a modified Green-Ampt equation which approximately accounts for the early resistive regime. *Wang et al*. [1997] derived an explicit expression for the entire period of infiltration with air compression and counterflow. *Sabeh* [2004] modified the original Green-Ampt model to consider air compression and counterflow. Infiltration, air compression, and counterflow in the model were decoupled within a time step, and air counterflow was calculated as a mass flux [*Charbeneau*, 2000]. On the basis of the original Green-Ampt model and *Sabeh*'s [2004] infiltration model, which accounts for air compression and air counterflow, *Lukyanets* [2010] developed a modified Green-Ampt model for modeling the infiltration process during postponding conditions. In the model, air counterflow, air compression, and infiltration were decoupled and updated with each wetting front increment [*Lukyanets*, 2010]. The possibility of extending the equations to nonuniform porous media was mentioned by *Wang et al*. [1997]. *Ma et al*. [2011] developed a modified Green-Ampt model to account for the effect of entrapped air on infiltration in layered soils.

[94] Some researchers also derived modified Green-Ampt models for infiltration with air effect from an air-water two-phase flow point of view. Using an air-water two-phase flow analysis, *Morel-Seytoux and Khanji* [1974] derived an infiltration equation considering the viscous resistance to simultaneous flow of water and air. On the basis of the work of *Morel-Seytoux and Khanji* [1974], *Morel-Seytoux and Khanji* [1975] added the compression and counterflow effects to the model of *Morel-Seytoux and Khanji* [1974] and derived equations accounting for air compression effect and accounting for both air compression and counterflow effects, respectively.

5.2.2. Air-Water Two-Phase Flow Model

[95] In the infiltration process, water enters the porous material under the influence of gravitational and capillary forces. This process always involves the displacement of air by water [*McWhorter*, 1971; *van Phuc and Morel-Seytoux*, 1972; *Youngs*, 1995]. Thus, the process of water infiltration is an air-water two-phase flow problem [e.g., *Brustkern and Morel-Seytoux*, 1970; *McWhorter*, 1971]. *Vachaud et al*. [1973] illustrated the inadequacy of the one-phase flow approach to describe the infiltration process in a vertical stratified column of sand when the air phase cannot escape freely and suggested that the flow equations must be written in terms of two-phase immiscible fluid flow. *van Phuc and Morel-Seytoux* [1972] found that the air pressure buildup is present even for a semi-infinite medium. *Morel-Seytoux and Billica* [1985a] presented that the two-phase flow approach is indeed needed even for a semi-infinite soil column when mobile air cannot be confined. *Navarro et al*. [2008] demonstrated quantitatively the suitability of use of an air-water two-phase flow model. The results show that in the clayey soils analyzed, the soil air pressure is 22% greater than the atmospheric pressure, and the water intake rate is only 19% of the values that would have been obtained if free air escape is considered (no air compression).

[96] The equations which describe the air-water two-phase flow problem are based on the following assumptions [*McWhorter*, 1971; *Vachaud et al*., 1973; *Vauclin*, 1989]: (1) Darcy's law is valid and can be applied to both water and air; (2) the porous medium is homogeneous and isotropic; (3) the physical properties of the porous medium are constant; (4) the two fluids are homogeneous and immiscible, and their viscosities are constant; and (5) water is incompressible and air is compressible.

[97] The equations of mass conservation for both water and air can be written as

$$\frac{\partial}{\partial t}(\rho_w \theta_w) = -\frac{\partial}{\partial z}(\rho_w q_w) \tag{11}$$

$$\frac{\partial}{\partial t}(\rho_a \theta_a) = -\frac{\partial}{\partial z}(\rho_a q_a) \tag{12}$$

where ϕ is the porosity of the porous medium, θ_w and θ_a are the volumetric water and air contents, respectively, $\theta_a + \theta_w = \phi$, ρ_w and ρ_a are the water and air densities, and q_w and q_a are the water and air volumetric fluxes. Equations (11) and (12) are the governing equations for isothermal one-dimensional air-water two-phase flow in porous medium, which are a coupled set of nonlinear partial differential equations [e.g., *Morel-Seytoux*, 1971; *van Phuc and Morel-Seytoux*, 1972; *Touma and Vauclin*, 1986; *Weir and Kissling*, 1992]. The general governing equations for simultaneous flow of air and water can also be found in the literature [e.g., *Bear*, 1972; *Celia and Binning*, 1992]. For the air-water two-phase immiscible fluid flow, water is the wetting phase and air is the nonwetting phase. The air and water volumetric fluxes are given by the Darcy's law generalized to both phases

$$q_w = -\frac{kk_{rw}}{\mu_w}\left(\frac{\partial p_w}{\partial z} - \rho_w g\right) \tag{13}$$

$$q_a = -\frac{kk_{ra}}{\mu_a}\left(\frac{\partial p_a}{\partial z} - \rho_a g\right) \tag{14}$$

where k is the intrinsic permeability of the porous medium, k_{rw} and k_{ra} are the relative permeability of the porous medium to water and air, respectively, μ_w is the water viscosity, p_w is the water pressure, and g is the gravitational acceleration. The vertical coordinate z is oriented positive downward. Equations (13) and (14) are the generalized Darcy's law for air-water two-phase flow in the vertical direction [e.g., *Morel-Seytoux*, 1971; *Brustkern and Morel-Seytoux*, 1970; *Noblanc and Morel-Seytoux*, 1972; *van Phuc and Morel-Seytoux*, 1972; *Touma and Vauclin*, 1986; *Weir and Kissling*, 1992]. The capillary pressure is defined as the difference between the air pressure and water pressure, which can be written as [e.g., *McWhorter*, 1971; *Morel-Seytoux*, 1971; *Bear*, 1972]

$$p_c = p_a - p_w \tag{15}$$

[98] Given equations (11)–(15), the following relationships must be provided

$$k_{rw} = k_{rw}(\theta_w) \tag{16}$$

$$k_{ra} = k_{ra}(\theta_w) \tag{17}$$

$$p_c = p_c(\theta_w) \tag{18}$$

$$\rho_a = \rho_a(p_a) \tag{19}$$

The relative permeability functions and the capillary pressure-saturation relationship are usually determined by experiment. Air is assumed to be a perfect gas, and its density is a function of the air pressure p_a [e.g., *Touma and Vauclin*, 1986; *Vauclin*, 1989; *Celia and Binning*, 1992]. Equations (11)–(19) constitute a set of simultaneous equations which can be solved when appropriate initial and boundary conditions are specified [*McWhorter*, 1971].

[99] The governing equations are nonlinear partial differential equations, no exact analytical solutions are known in the literature [e.g., *van Phuc and Morel-Seytoux*, 1972; *Touma and Vauclin*, 1986]. *Morel-Seytoux* [1973] presented an excellent development of the various forms of the two-phase flow governing equations under different conditions. *Vauclin* [1989] reviewed various quasianalytical and numerical solutions of the air-water two-phase flow problem and compared them with experimental data. *Kuang et al*. [2011] presented a brief review of two-phase flow analytical and numerical models.

[100] Various analytical or quasianalytical solutions have been derived to describe the flow of air and water during infiltration. *Brustkern and Morel-Seytoux* [1970] presented a procedure for analyzing the infiltration problem using air-water two-phase flow approach. The procedure is largely analytic and the calculated infiltration rates compare favorably with those by a finite difference solution. In the solution, air was assumed to be incompressible. While *Brustkern and Morel-Seytoux* [1970] emphasized the prediction of infiltration rates, *Brustkern and Morel-Seytoux* [1975] developed an approximate analytical solution for the problem of infiltration into a homogeneous porous medium with emphasis on the determination of the saturation profile during infiltration. On the basis of the work of *Brustkern and Morel-Seytoux* [1970], *Noblanc and Morel-Seytoux* [1972] considered the influence of capillarity on the shape of the saturation profile and added a perturbation term to the *Brustkern and Morel-Seytoux*'s [1970] equation. *Sonu and Morel-Seytoux* [1976] derived equations to predict infiltration rate, evolution of water content, and the evolution of water table in a soil under natural hydrological boundary conditions. Using a two-phase flow approach, analytical results were obtained to predict infiltration under conditions of constant and variable rainfall by *Morel-Seytoux* [1976, 1978, 1982]. *Morel-Seytoux* [1983] summarized some previous work on the effects of air entrapment, air viscous resistance, air confinement, and air compression on infiltration.

[101] Furthermore, *McWhorter* [1971] investigated theoretically and experimentally the problem of infiltration subject to various boundary conditions. The effect of air counterflow was included in the analysis. *Parlange and Hill* [1979] extended *McWhorter*'s [1971] analysis by considering the effect of air compressibility to study the flow of air and water in a sand column. Following the approach of *McWhorter* [1971], *Sander and Parlange* [1984] derived an analytical approximation for the water profile in a soil with the air effects considered using a Brutsaert-type profile and optimization techniques. On the basis of *McWhorter*'s [1971] work, *Sander et al*. [1988] presented an approximate solution for one-dimensional gravitational air and water flows in a porous medium under arbitrary flux boundary condition.

[102] In numerical solutions of the two-phase flow problem, specific expressions for $p_c(\theta_w)$, $k_{rw}(\theta_w)$, and $k_{ra}(\theta_w)$ must be specified. The van Genuchten-Mualem (VGM) [*van Genuchten*, 1980; *Mualem*, 1976] model is frequently used by researchers and can be expressed as

$$p_c(\theta_w) = p_0\left(S_{ew}^{-1/m} - 1\right)^{1/n} \tag{20}$$

$$k_{rw}(\theta_w) = S_{ew}^{1/2}\left[1 - \left(1 - S_{ew}^{1/m}\right)^m\right]^2 \tag{21}$$

$$k_{ra}(\theta_w) = (1 - S_{ew})^{1/2}\left(1 - S_{ew}^{1/m}\right)^{2m} \tag{22}$$

where S_{ew} is the effective water saturation given by $S_{ew} = (\theta_w - \theta_{rw})/(\theta_{sw} - \theta_{rw})$, in which θ_{rw} and θ_{sw} are the residual and saturated volumetric water contents, respectively, $p_0 = \rho_w g/\alpha$, α, n, and m are parameters obtained from fitting equation (20) to experimental data with the constraint $m = 1 - 1/n$ [*van Genuchten*, 1980]. Equation (22) was presented by *Parker et al*. [1987]. Many capillary pressure-saturation relationships (soil water characteristic curve or soil water retention curve) can be found in the literature [e.g., *van Genuchten and Nielsen*, 1985; *Fredlund*

and Xing, 1994; *Leij et al*., 1997; *Leong and Rahardjo*, 1997a; *Singh*, 1997; *Assouline et al*., 1998, 2000; *Sillers et al*., 2001]. Correspondingly, there are lots of relative water permeability models in the literature [e.g., *Mualem*, 1986; *Leong and Rahardjo*, 1997b; *Assouline*, 2001, 2004]. For the relative air permeability models, *Dury et al*. [1999] presented a comparison of the models that exist in the literature against experimental data. A summary of various relative air permeability models was given by *Chen et al*. [1999] and *Kuang and Jiao* [2011]. In modeling the infiltration process using a two-phase flow approach, hysteresis in the constitutive relationships [e.g., *Youngs and Peck*, 1964; *Morel-Seytoux*, 1973; *Vachaud et al*., 1974; *Haverkamp and Parlange*, 1986; *Scott et al*., 1983; *Touma and Vauclin*, 1986; *Kool and Parker*, 1987; *Kaluarachchi and Parker*, 1987; *Parker and Lenhard*, 1987; *Luckner et al*., 1989; *Parker*, 1989; *Muccino et al*., 1998] may also be considered.

[103] A variety of numerical models were developed to simulate the air-water two-phase flow infiltration problem. *van Phuc and Morel-Seytoux* [1972] presented a numerical solution of the equations describing the simultaneous flow of air and water in a soil using the finite difference method. *Morel-Seytoux and Billica* [1985a] presented a numerical algorithm for the prediction of infiltration and water content profiles evolution in a semi-infinite soil column using the finite difference method. On the basis of the work of *Morel-Seytoux and Billica* [1985a], *Morel-Seytoux and Billica* [1985b] considered air compression and presented a numerical algorithm for prediction of infiltration in a column with an impervious bottom. *Touma and Vauclin* [1986] solved the air-water two-phase flow problem in the vertical direction using an implicit finite difference scheme and modeled the infiltration experiments using the solution. *Celia and Binning* [1992] presented a mass conservative numerical solution for two-phase flow in porous media and applied the solution to simulate the infiltration experiments conducted by *Touma and Vauclin* [1986]. *Weir and Kissling* [1992] investigated numerically and analytically the vertical flow of air and water into a Gardner soil. *Felton and Reddell* [1992] developed a two-dimensional transient finite element solution of air-water two-phase flow and simulated the effects of air compression and counterflow on infiltration. Using a finite element method, *Navarro et al*. [2008] presented a two-dimensional two-phase flow model to account for the effects of air compression on infiltration in clays during flood irrigation. Well-documented software is also available to simulate air-water two-phase flow in porous media, such as FEHM [*Zyvoloski et al*., 1988; *Dash*, 2005] and TOUGH2 [*Pruess et al*., 1999]. A summary of such software is given by *Scanlon et al*. [2002].

5.3. Lisse Effect

[104] Air pressure buildup induced by infiltration between the wetting front and the water table can cause an apparent rise in the water table [*Bianchi and Haskell*, 1966; *Meyboom*, 1967; *Linden and Dixon*, 1973; *Heliotis and DeWitt*, 1987]. The Lisse effect is a phenomenon occurring when infiltration caused by intensive rainfall seals the surface soil layer to airflow, trapping and compressing air in the unsaturated zone; the pressure increase produces a very rapid water level rise in an observation well screened below the water table [*Weeks*, 2002]. It was first noted and explained by Thal Larsen in 1932 from water level observations obtained in a shallow well located in the village of Lisse, Holland. The effect is induced by intense rains and results in a rapid water level rise, followed by a recession lasting for several hours to a few days. A comprehensive analysis of the Lisse effect is presented by *Weeks* [2002].

[105] The water level rise caused by the Lisse effect is typically ranges from 0.10 to 0.55 m [*Weeks*, 2002]. It is usually over an order of magnitude larger than the amount of rainfall. An example of the Lisse effect, provided by *Meyboom* [1967], is shown in Figure 11. The water level rose from 1.35 m below the measuring point to about 0.82 m below the measuring point due to the Lisse effect, giving a water level rise of 0.53 m. The ratio of rainfall to water level rise is equal to 1:18.5. *Meyboom* [1967] observed that the relation between rainfall and water level rise is commonly of the order of 1:18. *Heliotis and DeWitt* [1987] identified 20 occurrences of the Lisse effect in four observation wells located in a lakeshore cedar swamp based on the established qualitative criteria among 200 water level responses to rainfall and concluded from the observations of water level rise that the ratio of water level rise to rainfall ranges from 10.8 to 33.0. *Weeks* [2002] presented that the ratio of water level rise to amount of rain producing the rise is typically ranges from 20 to 50.

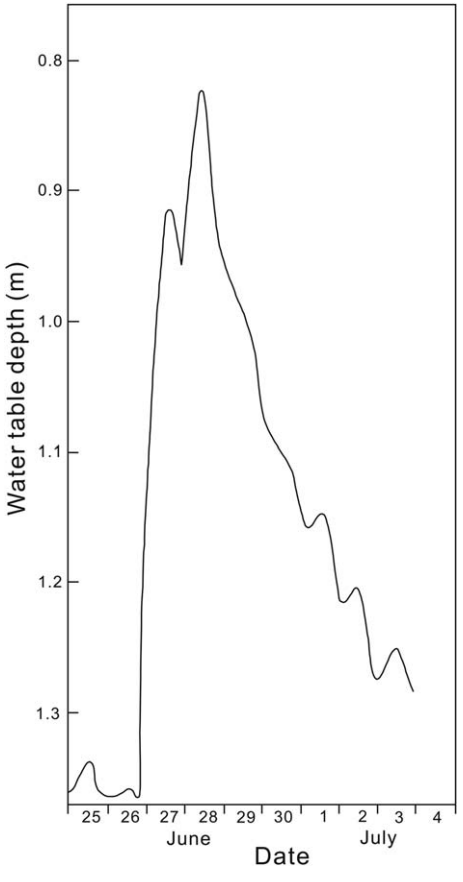

Figure 11. Example of the Lisse effect (modified from *Meyboom* [1967]). Water table depth was measured as meters below measuring point.

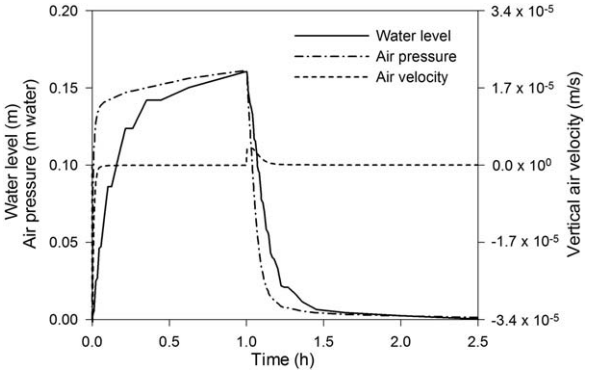

Figure 12. Time evolution of the water level in the observation well, the vertical air velocity, and the air pressure at a point 0.41 m below the ground surface (modified from *Guo et al*. [2008]). Ponded infiltration was assumed in the simulation. The ponding depth was assumed to be 0.06 m and duration of the ponding was assumed to be 1 h.

[106] *Guo et al*. [2008] set up a transient three-dimensional air-water two-phase flow numerical model to predict the magnitude of the Lisse effect in modeled conditions that mimic the physical complexity of real aquifers. Figure 12 shows the simulated variation of the water level in the observation well with time. The rate of water level rise is most significant during the first 20 min of ponding. It reaches a maximum of 0.16 m at the time ponding stops. The water level recovers quickly when ponding stops at 1 h. However, the rate of recovery decreases after about 1.45 h. It can also be seen that the water level rise is delayed relative to the air pressure buildup in the unsaturated zone. This kind of delayed response may be attributed to the effects of wellbore storage [*Guo et al*., 2008].

[107] Figure 12 also shows the time evolution of the simulated air pressure at a point 0.41 m below the ground surface and the vertical air velocity. For the vertical air velocity, there are two peaks which approximately correspond with the time when ponding starts and stops, respectively. At the very beginning of the ponding, air is driven into the soil as a result of water infiltration. This increases the soil air pressure and the water level rises quickly. The soil air pressure and the water level then rise slowly. When ponding is removed at 1 h, the flow is reversed and air escapes quickly back to the atmosphere with a dramatic decrease in the pressure. Meanwhile, the water level falls significantly. When the vertical air velocity drops to zero again, the water level falls slowly [*Guo et al*., 2008].

[108] The occurrence of the Lisse effect depends on several factors, namely, soil pore size, water table depth, rain magnitude, ponding depth, soil permeability, and air entry pressure [*Meyboom*, 1967; *Heliotis and DeWitt*, 1987; *Weeks*, 2002; *Guo et al*., 2008]. *Meyboom* [1967] concluded that the optimum condition for the Lisse effect to occur is that the water table depth is about 0.6 m below ground surface. When the water table is deeper than about 1.2 m, the Lisse effect was never observed to occur [*Meyboom*, 1967]. *Heliotis and DeWitt* [1987] conducted extensive laboratory experiments on soil cores to examine the effects of water table depth and rain magnitude on the Lisse effect. Results show that when the initial water table depth is less than a critical value, immediate large responses of water level always occurred. For depth greater than the critical value, only gradual water level rises were observed, and the rises can be predicted from specific yield. Results also show that too small rain magnitude does not result in rapid water level rise for any water table depth. *Weeks* [2002] stated that the water level rise caused by the Lisse effect is limited by the air entry pressure of the porous medium containing the wetting front. When the soil air pressure (relative to atmospheric pressure) exceeds the water pressure head above the wetting front by an amount equal to the bubbling pressure (minus the air entry pressure) of the medium, air entrapped beneath the wetting front will begin to escape. *Guo et al*. [2008] concluded from numerical modeling results that the magnitude of Lisse effect increases with air entry pressure, ponding depth, and soil permeability; decreases with pore size distribution and water table depth. The air entry pressure and ponding depth have the most significant impact on the Lisse effect [*Guo et al*., 2008].

[109] However, the Lisse effect is a rarely noted phenomenon and likely is not observable in most field situations because of land surface irregularities, macropores, unstable wetting fronts, and fingering [e.g., *Dixon and Peterson*, 1971; *Beven and Germann*, 1982; *Heliotis and DeWitt*, 1987]. For example, irregularities in land surface would result in an irregular wetting front of variable thickness that would allow air to escape from areas of thinnest wetting

Table 3. Similarities and Differences of the Naturally Induced Airflows

Natural Forcings	Atmospheric Pressure Fluctuations	Topographic Effect	Water Table Fluctuations	Infiltration
Duration of pressure fluctuation	Diurnal, several days, and seasonal	Seasonal	Diurnal and semidiurnal	Hourly and diurnal
Magnitude of pressure fluctuation	−3.0 to 3.0 kPa	0.007–0.75 kPa	−5.0 to 5.0 kPa	1.0–10.0 kPa
Propagation depth	Several meters to over 10 m in porous media, up to over 100 m in fractured media	Up to over 1000 m	Thickness of the unsaturated zone	Thickness of the unsaturated zone
Applications	Air permeability estimation, passive soil vapor extraction, passive bioventing, radon transport, carbon dioxide transport, water vapor transport, and other trace gases transport	Unsaturated zone gas transport, mine natural ventilation, and tunnel natural ventilation	Air permeability estimation, environmental remediation, and coastal soil aeration	Rainfall infiltration, irrigation, and groundwater recharge

front thickness; macropores often extend to land surface and allow air to escape after the finer pores are sealed to airflow by the wetting front. The Lisse effect requires so ideal conditions to occur that they are rarely met in nature [*Weeks*, 2002]. It may be more appropriately treated as a scientific curiosity than as a significant hydrologic phenomenon because of its rarity [*Weeks*, 2002]. However, failure to recognize the phenomenon might result in overestimation of groundwater recharge [*Healy and Cook*, 2002]. It may also impede infiltration and subsequently increase runoff during intense rains [*Healy and Cook*, 2002; *Weeks*, 2002].

6. Similarities and Differences of the Naturally Induced Airflows

[110] In this section, the similarities and differences of the naturally induced airflows are compared and discussed. A comparison of the airflow induced by the various natural forcings is shown in Table 3. One of the common features is the duration of the pressure fluctuations, except the pressure fluctuation induced by topographic effect. The airflow induced by topographic effect is basically seasonal, while others share the diurnal flow pattern. In Table 3, the magnitude of pressure fluctuation is the common range of the pressure fluctuations. Under certain conditions, the pressure fluctuation can be larger than the upper limit or smaller than the lower limit. The largest magnitude of pressure fluctuation is the pressure fluctuation induced by infiltration, which can be 10.0 kPa or more. The smallest one is that induced by topographic effect, which can be only several Pascals. Although the magnitude of air pressure fluctuation induced by topographic effect is relatively small, this is the kind of airflow that can propagate very deep. For example, in mines, its propagation depth depends on the depth of the mine. For the airflow induced by water table fluctuations and infiltration, the propagation depth of the flow is the whole thickness of the unsaturated zone. This is due to the fact that the flow occurs between the water table and the ground surface. Furthermore, Table 3 shows that all kinds of the induced airflows have important applications.

7. Future Research

[111] While much progress has been made in the development of theoretical models, and many experiments have been done to investigate the naturally induced subsurface airflow, many unresolved problems remain. Some of the unresolved problems are summarized as follows. Because of the importance of greenhouse gases (carbon dioxide, methane, and water vapor) in regulating global climate change, it is very important to quantify the fluxes of these gases in response to atmospheric pressure fluctuations. Meanwhile, although numerous investigations have been conducted to interpret the effects of atmospheric pressure changes on soil gas radon concentration and transport of radon from soil to air, the role of atmospheric pressure changes on radon emission is still an open question. Hence, special attention should also be given to this topic in the future. Furthermore, it is also important to investigate the effects of atmospheric pressure fluctuations on transport of gases from cracked soil or fractured rock to atmosphere. Attention should also be given to using advanced two-phase flow theory to analyze rainfall infiltration both in the field and in the laboratory. New insights should be obtained in the infiltration process with the newly developed soil water retention equation, relative permeability model, and air-water two-phase flow numerical models.

8. Summary and Conclusions

[112] Subsurface airflow induced by various natural forcings including atmospheric pressure fluctuations, topographic effect, water table fluctuations, and infiltration is reviewed in this paper. The present state of knowledge on the induced airflow is presented, and applications of the induced airflow are also discussed. Airflow induced by atmospheric pressure fluctuations is most common and has been studied the most because of its important application in environmental remediation and transport of trace gases from soil to atmosphere. Airflow induced by infiltration has also been extensively investigated because of its important implications in rainfall infiltration, irrigation, and groundwater recharge. Airflow induced by water table fluctuations is a relatively new topic and research on this topic is limited. However, this area of research deserves more attention because of its potential effects on coastal environmental remediation and the coastal ecological system. Airflow induced by topographic effect is studied the least, but it has important applications in unsaturated zone gas transport and natural ventilation of mines and tunnels.

[113] **Acknowledgments.** The authors thank the reviewers for their insightful and helpful comments. This research was supported by the Research Grants Council of the Hong Kong Special Administrative Region, China (HKU 701908P). The authors thank J. Rossabi for providing measured data used in Figure 1.

References

Abbas, T. R. (2011), Effect of water table fluctuation on barometric pumping in soil unsaturated zone, *Jordan J. Civ. Eng.*, *5*(4), 504–509.

Adrian, D. D., and J. B. Franzini (1966), Impedance to infiltration by pressure build-up ahead of the wetting front, *J. Geophys. Res.*, *71*(24), 5857–5862.

Ahlers, C. F., S. Finsterle, and G. S. Bodvarsson (1999), Characterization and prediction of subsurface pneumatic response at Yucca Mountain, Nevada, *J. Contam. Hydrol.*, *38*(1–3), 47–68.

Albert, M. R. (1996), Modeling heat, mass, and species transport in polar firn, *Ann. Glaciol.*, *23*, 138–143.

Albert, M. R., and W. R. McGilvary (1992), Thermal effects due to air flow and vapor transport in dry snow, *J. Glaciol.*, *38*(129), 273–281.

Albert, M. R., and E. F. Shultz (2002), Snow and firn properties and air-snow transport processes at Summit, Greenland, *Atmos. Environ.*, *36*(15–16), 2789–2797.

Albert, M. R., A. M. Grannas, J. Bottenheim, P. B. Shepson, F. E. Perron (2002), Processes and properties of snow-air transfer in the high Arctic with application to interstitial ozone at Alert, *Canada, Atmos. Environ.*, *36*(15–16), 2779–2787.

Andersen, C. E. (2000), *Radon Transport Modelling: User's Guide to RnMod3d, Risø-R-1201(EN)*, Risø National Lab., *Roskilde, Denmark.*

Assouline, S. (2001), A model for soil relative hydraulic conductivity based on the water retention characteristic curve, *Water Resour. Res.*, *37*(2), 265–271.

Assouline, S. (2004), Correction to "A model for soil relative hydraulic conductivity based on the water retention characteristic curve," *Water Resour. Res.*, *40*, W02901, doi:10.1029/2004WR003025.

Assouline, S., D. Tessier, and A. Bruand (1998), A conceptual model of the soil water retention curve, *Water Resour. Res.*, *34*(2), 223–231.

Assouline, S., D. Tessier, and A. Bruand (2000), Correction to ''A conceptual model of the soil water retention curve'' by S. Assouline, D. Tessier, and A. Braund, *Water Resour. Res.*, *36*(12), 3769.

Auer, L. H., N. D. Rosenberg, K. H. Birdsell, and E. M. Whitney (1996), The effects of barometric pumping on contaminant transport, *J. Contam. Hydrol.*, *24*(2), 145–166.

Baldocchi, D. D., and T. P. Meyers (1991), Trace gas exchange above the floor of a deciduous forest: 1. Evaporation and CO_2 efflux, *J. Geophys. Res.*, *96*(D4), 7271–7285.

Baver, L. D., W. H. Gardner, and W. R. Gardner (1972), *Soil Physics*, 4th ed., John Wiley, New York.

Bear, J. (1972), *Dynamics of Fluids in Porous Media*, Elsevier, New York.

Beven, K., and P. Germann (1982), Macropores and water flow in soils, *Water Resour. Res.*, *18*(5), 1311–1325.

Bianchi, W. C., and E. E. Haskell Jr. (1966), Air in the vadose zone as it affects water movements beneath a recharge basin, *Water Resour. Res.*, *2*(2), 315–322.

Bobo, A. M., N. Khoury, H. Li, and M. C. Boufadel (2012), Groundwater flow in a tidally influenced gravel beach in Prince William Sound, Alaska, *J. Hydrol. Eng.*, *17*(4), 478–494.

Bond, W. J., and N. Collis-George (1981), Ponded infiltration into simple soil systems: 1. The saturation and transition zones in the moisture content profiles, *Soil Sci.*, *131*(4), 202–209.

Börjesson, G., and B. H. Svensson (1997), Seasonal and diurnal methane emissions from a landfill and their regulation by methane oxidation, *Waste Manage. Res.*, *15*(1), 33–54.

Bouwer, H. (1964), Unsaturated flow in ground-water hydraulics, *J. Hydraul. Div.*, *90*(HY5), 121–144.

Bouwer, H. (1966), Rapid field measurement of air entry value and hydraulic conductivity of soil as significant parameters in flow system analysis, *Water Resour. Res.*, *2*(4), 729–738.

Bouwer, H. (1969), Infiltration of water into nonuniform soil, *J. Irrig. Drain. Div.*, *95*(IR4), 451–461.

Brakensiek, D. L. (1977), Estimating the effective capillary pressure in the Green and Ampt infiltration equation, *Water Resour. Res.*, *13*(3), 680–682.

Brustkern, R. L., and H. J. Morel-Seytoux (1970), Analytical treatment of two-phase infiltration, *J. Hydraul. Div.*, *96*(HY12), 2535–2548.

Brustkern, R. L., and H. J. Morel-Seytoux (1975), Description of water and air movement during infiltration, *J. Hydrol.*, *24*(1–2), 21–35.

Buckingham, E. (1904), Contributions to our knowledge of the aeration of soils, *Soils Bull.*, *25*, 5–52.

Camp Dresser and McKee (1986), Investigation, analyses, and numerical simulation of subsurface vapor transport, Document prepared for the U.S. Environ. Prot. Agency under Contract 68-01-6939, Boston, Mass.

Carr, P. A. (1971), Use of harmonic analysis to study tidal fluctuations in aquifers near the sea, *Water Resour. Res.*, *7*(3), 632–643.

Carslaw, H. S., and J. C. Jaeger (1959), *Conduction of Heat in Solids*, 2nd ed., Clarendon, Oxford, U. K.

Cary, J. W. (1967), The drying of soil: Thermal regimes and ambient pressures, *Agric. Meteorol.*, *4*(5), 353–365.

Celia, M. A., and P. Binning (1992), A mass conservative numerical solution for two-phase flow in porous media with application to unsaturated flow, *Water Resour. Res.*, *28*(10), 2819–2828.

Chang, T. Y., and S. J. Rudy (1990), Roadway tunnel air quality models, *Environ. Sci. Technol.*, *24*(5), 672–676.

Charbeneau, R. J. (2000), *Groundwater Hydraulics and Pollutant Transport*, Prentice Hall, Upper Saddle River, N. J.

Chen, C., D. M. Thomas, and R. E. Green (1995), Modeling of radon transport in unsaturated soil, *J. Geophys. Res.*, *100*(B8), 15,517–15,525.

Chen, J., J. W. Hopmans, and M. E. Grismer (1999), Parameter estimation of two-fluid capillary pressure-saturation and permeability functions, *Adv. Water Resour.*, *22*(5), 479–493.

Childs, E. C. (1969), *An Introduction to the Physical Basis of Soil Water Phenomena*, John Wiley, London, U. K.

Chiodini, G., R. Cioni, M. Guidi, B. Raco, and L. Marini (1998), Soil CO_2 flux measurements in volcanic and geothermal areas, *Appl. Geochem.*, *13*(5), 543–552.

Christensen, A. G., E. V. Fischer, H. H. Nielsen, T. Nygaard, H. Østergaard, S. R. Lenschow, H. Sørensen, I. A. Fuglsang, and T. H. Larsen (2000), Passive soil vapor extraction of chlorinated solvents using boreholes, in *Groundwater 2000*: Proceedings of the International Conference on Groundwater Research, Copenhagen, Denmark, 6–8 Jun. 2000, edited by P. L. Bjerg, P. Engesgaard, and T. D. Krom, pp. 409–410, A. A. Balkema, Rotterdam, Netherlands.

Christophersen, M., P. Kjeldsen, H. Holst, and J. Chanton (2001), Lateral gas transport in soil adjacent to an old landfill: Factors governing emissions and methane oxidation, *Waste Manage. Res.*, *19*(6), 595–612.

Clarke, G. K. C., and E. D. Waddington (1991), A three-dimensional theory of wind pumping, *J. Glaciol.*, *37*(125), 89–96.

Clarke, G. K. C., D. A. Fisher, and E. D. Waddington (1987), Wind pumping: A potentially significant heat source in ice sheets, in *The Physical Basis of Ice Sheet Modelling: Proceedings of the Vancouver Symposium, August 1987*, IAHS Publ., *170*, pp. 169–180.

Clements, W. E., and M. H. Wilkening (1974), Atmospheric pressure effects on ^{222}Rn transport across the earth-air interface, *J. Geophys. Res.*, *79*(33), 5025–5029.

Colbeck, S. C. (1989), Air movement in snow due to windpumping, *J. Glaciol.*, *35*(120), 209–213.

Colbeck, S. C. (1997), Model of wind pumping for layered snow, *J. Glaciol.*, *43*(143), 60–65.

Collis-George, N., and W. J. Bond (1981), Ponded infiltration into simple soil systems: 2. Pore air pressures ahead of and behind the wetting front, *Soil Sci.*, *131*(5), 263–270.

Constantz, J., W. N. Herkelrath, and F. Murphy (1988), Air encapsulation during infiltration, *Soil Sci. Soc. Am. J.*, *52*(1), 10–16.

Culligan, P. J., D. A. Barry, J.-Y. Parlange, T. S. Steenhuis, and R. Haverkamp (2000), Infiltration with controlled air escape, *Water Resour. Res.*, *36*(3), 781–785.

Cunningham, J., and E. D. Waddington (1993), Air flow and dry deposition of non-sea salt sulfate in polar firn: Paleoclimatic implications, *Atmos. Environ.*, *27A*(17–18), 2943–2956.

Czepiel, P. M., B. Mosher, R. C. Harriss, J. H. Shorter, J. B. McManus, C. E. Kolb, E. Allwine, and B. K. Lamb (1996), Landfill methane emissions measured by enclosure and atmospheric tracer methods, *J. Geophys. Res.*, *101*(D11), 16,711–16,719.

Czepiel, P. M., J. H. Shorter, B. Mosher, E. Allwine, J. B. McManus, R. C. Harriss, C. E. Kolb, and B. K. Lamb (2003), The influence of atmospheric pressure on landfill methane emissions, *Waste Manage.*, *23*(7), 593–598.

Dalgic, A., and A. Karakus (2004), A computerised study on the natural ventilation characteristics of the Guleman Kef chromium mine, *Min. Technol.*, *113*(3), 153–162.

Dash, Z. V. (2005), *Software Users Manual (UM) for the FEHM Application Version 2.30, 10086-UM-2.30-00*, Los Alamos Natl. Lab., Los Alamos, N. M.

Dixon, R. M., and D. R. Linden (1972), Soil air pressure and water infiltration under border irrigation, *Soil Sci. Soc. Am. Proc.*, *36*(6), 948–953.

Dixon, R. M., and A. E. Peterson (1971), Water infiltration vontrol: A channel system concept, *Soil Sci. Soc. Am. Proc.*, *35*(6), 968–973.

Dominé, F., and P. B. Shepson (2002), Air-snow interactions and atmospheric chemistry, *Science*, *297*(5586), 1506–1510.

Downs, W. C., Z. P. Walton, and P. A. Keddington (2000), Enhanced barometric pumping, in *Groundwater 2000: Proceedings of the International Conference on Groundwater Research*, Copenhagen, Denmark, 6–8 Jun. 2000, edited by P. L. Bjerg, P. Engesgaard, and T. D. Krom, pp. 363–364, A. A. Balkema, Rotterdam, Netherlands.

Dury, O., U. Fischer, and R. Schulin (1999), A comparison of relative nonwetting-phase permeability models, *Water Resour. Res.*, *35*(5), 1481–1493.

Edwards, J. C., and R. C. Bates (1980), Theoretical evaluation of radon emanation under a variety of conditions, *Health Phys.*, *39*(2), 263–274.

Eff-Darwich, A., C. Martín-Luis, M. Quesada, J. de laNuez, and J. Coello (2002), Variations on the concentration of ^{222}Rn in the subsurface of the volcanic island of Tenerife, Canary Islands, *Geophys. Res. Lett.*, *29*(22), 2069, doi:10.1029/2002GL015387.

Elberling, B., F. Larsen, S. Christensen, and D. Postma (1998), Gas transport in a confined unsaturated zone during atmospheric pressure cycles, *Water Resour. Res.*, *34*(11), 2855–2862.

Ellerd, M. G., J. W. Massmann, D. P. Schwaegler, and V. J. Rohay (1999), Enhancements for passive vapor extraction: The Hanford study, *Ground Water*, *37(3)*, 427–437.

Etiope, G., and G. Martinelli (2002), Migration of carrier and trace gases in the geosphere: An overview, *Phys. Earth Planet. Inter.*, *129*(3–4), 185–204.

Fairbanks, H. W. (1896), Note on a breathing gas well, *Science*, *3(71)*, 693–694.

Falta, R. W. (1996), A program for analyzing transient and steady-state soil gas pump tests, *Ground Water*, *34(4)*, 750–755.

Farrell, D. A., E. L. Greacen, and C. G. Gurr (1966), Vapor transfer in soil due to air turbulence, *Soil Sci.*, *102*(5), 305–313.

Felton, G. K, and D. L. Reddell (1992), A finite element axisymmetrical and linear model of two-phase flow through porous media, *Trans. ASAE*, *35(5)*, 1419–1429.

Ferris, J. G., D. B. Knowles, R. H. Brown, and R. W. Stallman (1962), Theory of Aquifer Test, *U. S. Geol. Surv. Water Supply Pap.*, 1536-E.

Fleischer, R. L., and A. Mogro-Campero (1979), Radon enhancements in the earth: Evidence for intermittent upflows?, *Geophys. Res. Lett.*, *6*(5), 361–364.

Foor, D. C., T. C. Zwick, R. E. Hinchee, R. E. Hoeppel, C. Kyburg, and L. Bowling (1995), Passive bioventing driven by natural air exchange, in *In Situ Aeration: Air Sparging, Bioventing, and Related Remediation Processes*, edited by R. E. Hinchee, R. N. Miller, and P. C. Johnson, pp. 369–375, Battelle Press, Columbus, Ohio.

Fredlund, D. G., and A. Xing (1994), Equations for the soil-water characteristic curve, *Can. Geotech. J.*, *31*(4), 521–532.

Free, G. R., and V. J. Palmer (1941), Interrelationship of infiltration, air movement, and pore size in graded silica sand, *Soil Sci. Soc. Am. Proc.*, *5*, 390–398.

Freeze, R. A., and J. A. Cherry (1979), *Groundwater*, Prentice Hall, Englewood Cliffs, N. J.

Fukuda, H. (1955), Air and vapor movement in soil due to wind gustiness, *Soil Sci.*, *79*(4), 249–256.

Galmarini, S. (2006), One year of ^{222}Rn concentration in the atmospheric surface layer, *Atmos. Chem. Phys.*, *6*, 2865–2886.

Gebert, J., and A. Groengroeft (2006), Passive landfill gas emission-influence of atmospheric pressure and implications for the operation of methane-oxidising biofilters, *Waste Manage.*, *26*(3), 245–251.

Gjessing, Y. T. (1977), The filtering effect of snow, in *Isotopes and Impurities in Snow and Ice: Proceedings of the Symposium at Grenoble 1975*, IAHS Publ., *118*, pp. 199–203.

Glaser, P. H., J. P. Chanton, P. Morin, D. O. Rosenberry, D. I. Siegel, O. Ruud, L. I. Chasar, and A. S. Reeve (2004), Surface deformations as indicators of deep ebullition fluxes in a large northern peatland, *Global Biogeochem. Cycles*, *18*, GB1003, doi:10.1029/2003GB002069.

Granieri, D., G. Chiodini, W. Marzocchi, and R. Avino (2003), Continuous monitoring of CO_2 soil diffuse degassing at Phlegraean Fields (Italy): Influence of environmental and volcanic parameters, *Earth Planet. Sci. Lett.*, *212*(1–2), 167–179.

Green, W. H., and G. A. Ampt (1911), Studies on soil physics, 1, The flow of air and water through soils, *J. Agric. Sci.*, *4*, 1–24.

Grismer, M. E., M. N. Orang, V. Clausnitzer, and K. Kinney (1994), Effects of air compression and counterflow on infiltration into soils, *J. Irrig. Drain. Eng.*, *120*(4), 775–795.

Gross, M. G. (1990), *Oceanography: A View of the Earth*, 5th ed., Prentice Hall, Englewood Cliffs, N. J.

Guedalia, D., J.-L. Laurent, J. Fontan, D. Blanc, and A. Druilhet (1970), A study of radon 220 emanation from soils, *J. Geophys. Res.*, *75*(2), 357–369.

Guo, H., and J. J. Jiao (2010), Theoretical study of the impact of tide-induced airflow on hydraulic head in air-confined coastal aquifers, *Hydrol. Sci. J.*, *55*(3), 435–445.

Guo, H.-P., and J. J. Jiao (2008), Numerical study of airflow in the unsaturated zone induced by sea tides, *Water Resour. Res.*, *44*, W06402, doi:10.1029/2007WR006532.

Guo, H., J. J. Jiao, and H. Li (2010), Groundwater response to tidal fluctuation in a two-zone aquifer, *J. Hydrol.*, *381*(3–4), 364–371.

Guo, H., J. J. Jiao, and E. P. Weeks (2008), Rain-induced subsurface airflow and Lisse effect, *Water Resour. Res.*, *44*, W07409, doi:10.1029/2007WR006294.

Hammecker, C., A. C. D. Antonino, J. L. Maeght, and P. Boivin (2003), Experimental and numerical study of water flow in soil under irrigation in northern Senegal: Evidence of air entrapment, *Eur. J. Soil Sci.*, *54*(3), 491–503.

Hanks, R. J., and N. P. Woodruff (1958), Influence of wind on water vapor transfer through soil gravel, and straw mulches, *Soil Sci.*, *86*(3), 160–164.

Hartman, H. L., J. M. Mutmansky, R. V. Ramani, and Y. J. Wang (1997), *Mine Ventilation and Air Conditioning*, 3rd ed., John Wiley, New York.

Haverkamp, R., and J.-Y. Parlange (1986), Predicting the water-retention curve from particle-size distribution: 1. Sandy soils without organic matter, *Soil Sci.*, *142*(6), 325–339.

Healy, R. W., and P. G. Cook (2002), Using groundwater levels to estimate recharge, *Hydrogeol. J.*, *10*(1), 91–109.

Heliotis, F. D., and C. B. DeWitt (1987), Rapid water table responses to rainfall in a northern peatland ecosystem, *Water Resour. Bull.*, *23*(6), 1011–1016.

Herbst, M., T. Friborg, R. Ringgaard, and H. Soegaard (2011), Interpreting the variations in atmospheric methane fluxes observed above a restored wetland, *Agric. For. Meteorol.*, *151*(7), 841–853.

Hinkle, M. E. (1994), Environmental conditions affecting concentrations of He, CO_2, O_2 and N_2 in soil gases, *Appl. Geochem.*, *9*(1), 53–63.

Holford, D. J. (1994), *Rn3D: A Finite Element Code for Simulating Gas Flow and Radon Transport in Variably Saturated, Nonisothermal Porous Media: User's Manual, Version 1.0*, PNL-8943, Pacific Northwest Lab., Richland, Wash.

Holford, D. J., S. D. Schery, J. L. Wilson, and F. M. Phillips (1993), Modeling radon transport in dry, cracked soil, *J. Geophys. Res.*, *98*(B1), 567–580.

Horton, R. E. (1941), An approach toward a physical interpretation of infiltration-capacity, *Soil Sci. Soc. Am. Proc.*, *5*, 399–417.

Hoover, H. C., and L. H. Hoover (1912), *Georgius Agricola de re* Metallica: translated from the Latin edition of 1556, reprinted 1950, Dover, New York.

Huang, C.-S., H.-D. Yeh, and C.-H. Chang (2012), A general analytical solution for groundwater fluctuations due to dual tide in long but narrow islands, *Water Resour. Res.*, *48*, W05508, doi:10.1029/2011WR011211.

Hutter, A. R. (1996), Spatial and temporal variations of soil gas ^{220}Rn and ^{222}Rn at two sites in New Jersey, *Environ. Int.*, *22*(S1), S455–S469.

Iakovleva, V. S., and N. K. Ryzhakova (2003), Spatial and temporal variations of radon concentration in soil air, *Radiat. Meas.*, *36*(1–6), 385–388.

Ishihara, Y., E. Shimojima, and H. Harada (1992), Water vapor transfer beneath bare soil where evaporation is influenced by a turbulent surface wind, *J. Hydrol.*, *131*(1–4), 63–104.

Jacob, C. E. (1950), Flow of ground water, in *Engineering Hydraulics*, edited by H. Rouse, pp. 321–386, John Wiley, New York.

Jarrett, A. R., and D. D. Fritton (1978), Effects of entrapped soil air on infiltration, *Trans. ASAE, 21*(5), 901–906.

Jennings, A. A., and P. Patil (2002), Feasibility modeling of passive soil vapor extraction, *J. Environ. Eng. Sci.*, *1*(2), 157–172.

Jiao, J. J., and H. Li (2004), Breathing of coastal vadose zone induced by sea level fluctuations, *Geophys. Res. Lett.*, *31*, L11502, doi:10.1029/2004GL019572.

Jiao, J. J., and Z. Tang (1999), An analytical solution of groundwater response to tidal fluctuation in a leaky confined aquifer, *Water Resour. Res.*, *35*(3), 747–751.

Kaluarachchi, J. J., and J. C. Parker (1987), Effects of hysteresis with air entrapment on water flow in the unsaturated zone, *Water Resour. Res.*, *23*(10), 1967–1976.

Kamath, R., D. T. Adamson, C. J. Newell, K. M. Vangelas, and B. B. Looney (2009), *Enhanced Attenuation Technologies: Passive Soil Vapor Extraction, Rev. 1.*, *SRNL-STI-2009-00571*, Savannah River Natl. Lab., Aiken, S. C.

Kataoka, T., et al. (2003), Concentrations of ^{222}Rn, its short-lived daughters and ^{212}Pb and their ratios under complex atmospheric conditions and topography, *Boundary Layer Meteorol.*, *107*(1), 219–249.

Katz, D. L., D. Cornell, R. Kobayashi, F. H. Poettmann, J. A. Vary, J. R. Elenbaas, and C. F. Weinaug (1959), *Handbook of Natural Gas Engineering*, McGraw-Hill, New York.

Kidder, R. E. (1957), Unsteady flow of gas through a semi-infinite porous medium, *J. Appl. Mech.*, *24*(3), 329–332.

Kimball, B. A., and E. R. Lemon (1971), Air turbulence effects upon soil gas exchange, *Soil Sci. Soc. Am. Proc.*, *35*(1), 16–21.

Kimball, B. A., and E. R. Lemon (1972), Theory of soil air movement due to pressure fluctuations, *Agric. Meteorol.*, *9*, 163–181.

Kipp, K. L., Jr. (1987), Effect of topography on gas flow in unsaturated fractured rock: Numerical simulation, in *Flow and Transport Through Unsaturated Fractured Rock*, edited by D. D. Evans, and T. J. Nicholson, pp. 171–176, AGU, Washington, D. C.

Kirkham, D. (1947), Field method for determination of air permeability of soil in its undisturbed state, *Soil Sci. Soc. Am. Proc.*, *11*, 93–99.

Klusman, R. W., and J. A. Jaacks (1987), Environmental influences upon mercury, radon and helium concentrations in soil gases at a site near Denver, Colorado, *J. Geochem. Explor.*, *27*(3), 259–280.

Koarashi, J., H. Amano, M. Andoh, and T. Iida (2000), Estimation of ^{222}Rn flux from ground surface based on the variation analysis of ^{222}Rn concentration in a closed chamber, *Radiat. Prot. Dosim.*, *87*(2), 121–131.

Kool, J. B., and J. C. Parker (1987), Development and evaluation of closed-form expressions for hysteretic soil hydraulic properties, *Water Resour. Res.*, *23*(1), 105–114.

Kovach, E. M. (1945), Meteorological influences upon the radon-content of soil-gas, *Trans. AGU*, *26(2)*, 241–248.

Kraner, H. W., G. L. Schroeder, and R. D. Evans (1964), Measurements of the effects of atmospheric variables on radon-222 flux and soil-gas concentrations, in *The Natural Radiation Environment*, pp. 191–215, Univ. of Chicago Press, Chicago, Ill.

Kuang, X., and J. J. Jiao (2011), A new model for predicting relative nonwetting phase permeability from soil water retention curves, *Water Resour. Res.*, *47*, W08520, doi:10.1029/2011WR010728.

Kuang, X., J. J. Jiao, L. Wan, X. Wang, and D. Mao (2011), Air and water flows in a vertical sand column, *Water Resour. Res.*, *47*, W04506, doi:10.1029/2009WR009030.

Larson, S. (2006), Design document for passive bioventing, *Naval Facil. Eng. Serv. Cent. Tech. Rep. ER-9715*, Port Hueneme, Calif.

Larson, S., and R. Hoeppel (2004), Cost and performance report for natural pressure-driven passive bioventing, *Naval Facil. Eng. Serv. Cent. Tech. Rep. TR-2253-ENV*, Port Hueneme, Calif.

Latifi, H., S. N. Prasad, and O. J. Helweg (1994), Air entrapment and water infiltration in two-layered soil column, *J. Irrig. Drain. Eng.*, *120*(5), 871–891.

Lehning, M., P. Bartelt, B. Brown, and C. Fierz (2002), A physical SNOWPACK model for the Swiss avalanche warning part III: Meteorological forcing, thin layer formation and evaluation, *Cold Reg. Sci. Technol.*, *35*(3), 169–184.

Leij, F. J., W. B. Russel, and S. M. Lesch (1997), Closed-form expressions for water retention and conductivity data, *Ground Water*, *35(5)*, 848–858.

Leong, E. C., and H. Rahardjo (1997a), Review of soil-water characteristic curve equations, *J. Geotech. Geoenviron. Eng.*, *123*(12), 1106–1117.

Leong, E. C., and H. Rahardjo (1997b), Permeability functions for unsaturated soils, *J. Geotech. Geoenviron. Eng.*, *123*(12), 1118–1126.

Leung, W. K., C. H. Li, and A. R. Pickles (2007), Heaving of airfield pavement at Hong Kong International Airport, 2007 FAA Worldwide Airport Technology Transfer Conference, Atlantic City, N. J., April 2007.

Lewicki, J. L., W. C. Evans, G. E. Hilley, M. L. Sorey, J. D. Rogie, and S. L. Brantley (2003), Shallow soil CO_2 flow along the San Andreas and Calaveras Faults, *California, J. Geophys. Res.*, *108*(B4), 2187, doi:10.1029/2002JB002141.

Lewicki, J. L., M. L. Fischer, and G. E. Hilley (2008), Six-week time series of eddy covariance CO_2 flux at Mammoth Mountain, California: Performance evaluation and role of meteorological forcing, *J. Volcanol. Geotherm. Res.*, *171*(3–4), 178–190.

Lewicki, J. L., G. E. Hilley, T. Tosha, R. Aoyagi, K. Yamamoto, and S. M. Benson (2007), Dynamic coupling of volcanic CO_2 flow and wind at the Horseshoe Lake tree kill, Mammoth Mountain, California, *Geophys. Res. Lett.*, *34*, L03401, doi:10.1029/2006GL028848.

Lewis, M. R., and W. L. Powers (1939), A study of factors affecting infiltration, *Soil Sci. Soc. Am. Proc.*, *3*, 334–339.

Li, H., and J. J. Jiao (2001), Tide-induced groundwater fluctuation in a coastal leaky confined aquifer system extending under the sea, *Water Resour. Res.*, *37*(5), 1165–1171.

Li, H., and J. J. Jiao (2005), One-dimensional airflow in unsaturated zone induced by periodic water table fluctuation, *Water Resour. Res.*, *41*, W04007, doi:10.1029/2004WR003916.

Li, H., J. J. Jiao, and M. Luk (2004), A falling-pressure method for measuring air permeability of asphalt in laboratory, *J. Hydrol.*, *286*(1–4), 69–77.

Li, H., J. J. Jiao, M. Luk, and K. Cheung (2002), Tide-induced groundwater level fluctuation in coastal aquifers bounded by L-shaped coastlines, *Water Resour. Res.*, *38*(3), 1024, doi:10.1029/2001WR000556.

Li, H., G. Li, J. Cheng, and M. C. Boufadel (2007), Tide-induced head fluctuations in a confined aquifer with sediment covering its outlet at the sea floor, *Water Resour. Res.*, *43*, W03404, doi:10.1029/2005WR004724.

Li, H., L. Li, and D. Lockington (2005), Aeration for plant root respiration in a tidal marsh, *Water Resour. Res.*, *41*, W06023, doi:10.1029/2004WR003759.

Li, J., K. You, H. Zhan, and G. Huang (2012a), Analytical solution to subsurface air pressure in a three-layer unsaturated zone with atmospheric pressure changes, *Transp. Porous Media*, *93*(3), 461–474.

Li, J., H. Zhan, G. Huang, and K. You (2011a), Tide-induced airflow in a two-layered coastal land with atmospheric pressure fluctuations, *Adv. Water Resour.*, *34*(5), 649–658.

Li, J., H. Zhan, G. Huang, and K. You (2012b), Determining air permeability in reclaimed coastal land based on tidal fluctuations, *Environ. Earth Sci.*, *66*(4), 1259–1268.

Li, H., Y. Zhang, and Y. Xia (2011b), An approximate analytical solution for measuring air permeability of asphalt samples partially saturated with water, *Environ. Earth Sci.*, *63*(2), 283–290.

Li, L., and D. A. Barry (2000), Wave-induced beach groundwater flow, *Adv. Water Resour.*, *23*(4), 325–337.

Linden, D. R., and R. M. Dixon (1973), Infiltration and water table effects of soil air pressure under border irrigation, *Soil Sci. Soc. Am. Proc.*, *37*(1), 94–98.

Linden, D. R., and R. M. Dixon (1976), Soil air pressure effects on route and rate of infiltration, *Soil Sci. Soc. Am. J.*, *40*(6), 963–965.

Linden, D. R., R. M. Dixon, and J. C. Guitjens (1977), Soil air pressure under successive border irrigations and simulated rain, *Soil Sci.*, *124*(3), 135–139.

Lindmark, A., and B. Rosen (1985), Radon in soil gas-exhalation tests and in situ measurements, *Sci. Total Environ.*, *45*, 397–404.

Lu, N. (1999), Time-series analysis for determining vertical air permeability in unsaturated zones, *J. Geotech. Geoenviron. Eng.*, *125*(1), 69–77.

Lu, N., and W. J. Likos (2004), *Unsaturated Soil Mechanics*, John Wiley, Hoboken, N. J.

Lu, N., E. M. Kwicklis, and J. P. Rousseau (2001), Determining fault permeability from subsurface barometric pressure, *J. Geotech. Geoenviron. Eng.*, *127*(9), 801–808.

Luckner, L., M. Th. van Genuchten, and D. R. Nielsen (1989), A consistent set of parametric models for the two-phase flow of immiscible fluids in the subsurface, *Water Resour. Res.*, *25*(10), 2187–2193.

Lukyanets, Y. (2010), The Green and Ampt infiltration model accounting for air compression and air counterflow in the shallow water table environment: Laboratory experiments, M.S. thesis, Univ. South Florida, Tampa, Fla.

Luo, Y., and X. Zhou (2006), *Soil Respiration and the Environment*, Elsevier/Academic, Amsterdam, Netherlands.

Ma, Y., S. Feng, D. Su, G. Gao, and Z. Huo (2010), Modeling water infiltration in a large layered soil column with a modified Green-Ampt model and HYDRUS-1D, *Comput. Electron. Agric.*, *71*(S1), S40–S47.

Ma, Y., S. Feng, H. Zhan, X. Liu, D. Su, S. Kang, and X. Song (2011), Water infiltration in layered soils with air entrapment: Modified Green-Ampt model and experimental validation, *J. Hydrol. Eng.*, *16*(8), 628–638.

Marmer, H. A. (1926), *The Tide*, D. Appleton and Company, New York.

Martinez, M. J., and R. H. Nilson (1999), Estimates of barometric pumping of moisture through unsaturated fractured rock, *Transp. Porous Media*, *36*(1), 85–119.

Massmann, J. W. (1989), Applying groundwater flow models in vapor extraction system design, *J. Environ. Eng.*, *115*(1), 129–149.

Massman, W. J. (2006), Advective transport of CO_2 in permeable media induced by atmospheric pressure fluctuations: 1. An analytical model, *J. Geophys. Res.*, *111*, G03004, doi:10.1029/2006JG000163.

Massmann, J., and D. F. Farrier (1992), Effects of atmospheric pressures on gas transport in the vadose zone, *Water Resour. Res.*, *28*(3), 777–791.

Massman, W. J., and J. M. Frank (2006), Advective transport of CO_2 in permeable media induced by atmospheric pressure fluctuations: 2. Observational evidence under snowpacks, *J. Geophys. Res.*, *111*, G03005, doi:10.1029/2006JG000164.

Massman, W., R. Sommerfeld, K. Zeller, T. Hehn, L. Hudnell, and S. Rochelle (1995), CO_2 flux through a Wyoming seasonal snowpack: diffusional and pressure pumping effects, in *Biogeochemistry of Seasonally Snow-Covered Catchments*, edited by K. A. Tonnessen, M. W. Williams, and M. Tranter, IAHS Publ., *228*, pp. 71–79.

Massman, W. J., R. A. Sommerfeld, A. R. Mosier, K. F. Zeller, T. J. Hehn, and S. G. Rochelle (1997), A model investigation of turbulence-driven pressure-pumping effects on the rate of diffusion of CO_2, N_2O, and CH_4 through layered snowpacks, *J. Geophys. Res.*, *102*(D15), 18,851–18,863.

Mattson, M. D., and G. E. Likens (1990), Air pressure and methane fluxes, *Nature*, *347*, 718–719.

McGee, K. A., and T. M. Gerlach (1998), Annual cycle of magmatic CO_2 in a tree-kill soil at Mammoth Mountain, California: Implications for soil acidification, *Geology*, *26*(5), 463–466.

McGee, K. A., T. M. Gerlach, R. Kessler, and M. P. Doukas (2000), Geochemical evidence for a magmatic CO_2 degassing event at Mammoth Mountain, California, September-December 1997, *J. Geophys. Res.*, *105*(B4), 8447–8456.

McWhorter, D. B. (1971), Infiltration affected by flow of air, *Colorado State Univ. Hydrol. Pap. 49*, Fort Collins, Colo.

Mein, R. G., and C. L. Larson (1973), Modeling infiltration during a steady rain, *Water Resour. Res.*, *9*(2), 384–394.

Meyboom, P. (1967), Groundwater studies in the Assiniboine River drainage basin, part II: Hydrologic characteristics of phreatophytic vegetation

in south-central Saskatchewan, *Geol. Surv. Can. Bull.*, *139*, Ottawa, Canada.

Meyers, T. P., and D. D. Baldocchi (1993), Trace gas exchange above the floor of a deciduous forest: 2. SO_2 and O_3 deposition, *J. Geophys. Res.*, *98*(D7), 12,631–12,638.

Miller, A., and J. C. Thompson (1970), *Elements of Meteorology*, Charles E. Merrill, Columbus, Ohio.

Montazer, P., E. P. Weeks, F. Thamir, D. Hammermeister, S. N. Yard, and P. B. Hofrichter (1988), Monitoring the vadose zone in fractured tuff, *Ground Water Monit. Rem.*, *8*(2), 72–88.

Morel-Seytoux, H. J. (1971), A systematic treatment of the problem of infiltration, *OWRR Completion Rep. Ser. 23*, Environ. Resour. Cent., Colorado State Univ., Fort Collins, Colo.

Morel-Seytoux, H. J. (1973), Two-phase flows in porous media, in *Advances in Hydroscience*, vol. *9*, edited by V. T. Chow, pp. 119–202, Academic, New York.

Morel-Seytoux, H. J. (1976), Derivation of equations for rainfall infiltration, *J. Hydrol.*, *31*(3–4), 203–219.

Morel-Seytoux, H. J. (1978), Derivation of equations for variable rainfall infiltration, *Water Resour. Res.*, *14*(4), 561–568.

Morel-Seytoux, H. J. (1982), Analytical results for prediction of variable rainfall infiltration, *J. Hydrol.*, *59*(3–4), 209–230.

Morel-Seytoux, H. J. (1983), Infiltration effected by air, seal, crust, ice and various sources of heterogeneity (special problems), in *Advances in Infiltration: Proceedings of the National Conference on Advances in Infiltration*, Hyatt Regency Illinois Center, Chicago, Illinois, 12–13 December, 1983, pp. 132–146, Am. Soc. of Agric. Eng., St. Joseph, Mich.

Morel-Seytoux, H. J., and J. A. Billica (1985a), A two-phase numerical model for prediction of infiltration: Applications to a semi-infinite soil column, *Water Resour. Res.*, *21*(4), 607–615.

Morel-Seytoux, H. J., and J. A. Billica (1985b), A two-phase numerical model for prediction of infiltration: Case of an impervious bottom, *Water Resour. Res.*, *21*(9), 1389–1396.

Morel-Seytoux, H. J., and J. Khanji (1974), Derivation of an equation of infiltration, *Water Resour. Res.*, *10*(4), 795–800.

Morel-Seytoux, H. J., and J. Khanji (1975), Equation of infiltration with compression and counterflow effects, *Hydrol. Sci. Bull.*, *20*(4), 505–517.

Morel-Seytoux, H. J., P. D. Meyer, M. Nachabe, J. Tourna, M. T. vanGenuchten and R. J. Lenhard (1996), Parameter equivalence for the Brooks-Corey and van Genuchten soil characteristics: Preserving the effective capillary drive, *Water Resour. Res.*, *32*(5), 1251–1258.

Moses, H., H. F. Lucas Jr., and G. A. Zerbe (1963), The effect of meteorological variables upon radon concentration three feet above the ground, *J. Air Pollut. Control Assoc.*, *13*(1), 12–19.

Mualem, Y. (1976), A new model for predicting the hydraulic conductivity of unsaturated porous media, *Water Resour. Res.*, *12*(3), 513–522.

Mualem, Y. (1986), Hydraulic conductivity of unsaturated soils: Prediction and formulas, in *Method of Soil Analysis, Part 1, Physical and Mineralogical Methods*, Agron. Monogr. 9, 2nd ed., pp. 799–823, Am. Soc. of Agron., Soil Sci. Soc. of Am., Madison, Wis.

Muccino, J. C., W. G. Gray, and L. A. Ferrand (1998), Toward an improved understanding of multiphase flow in porous media, *Rev. Geophys.*, *36*(3), 401–422.

Muskat, M. (1946), *The Flow of Homogeneous Fluids Through Porous Media*, J. W. Edwards, Ann Arbor, Mich.

Nachshon, U., M. Dragila, and N. Weisbrod (2012), From atmospheric winds to fracture ventilation: Cause and effect, *J. Geophys. Res.*, *117*, G02016, doi:10.1029/2011JG001898.

Nastev, M., R. Therrien, R. Lefebvre, and P. Gélinas (2001), Gas production and migration in landfills and geological materials, *J. Contam. Hydrol.*, *52*(1–4), 187–211.

Navarro, V., A. Yustres, M. Candel, and B. García (2008), Soil air compression in clays during flood irrigation, *Eur. J. Soil Sci.*, *59*(4), 799–806.

Nazaroff, W. W. (1992), Radon transport from soil to air, *Rev. Geophys.*, *30*(2), 137–160.

Neeper, D. A. (2002), Investigation of the vadose zone using barometric pressure cycles, *J. Contam. Hydrol.*, *54*(1–2), 59–80.

Neeper, D. A. (2003), Harmonic analysis of flow in open boreholes due to barometric pressure cycles, *J. Contam. Hydrol.*, *60*(3–4), 135–162.

Nielsen, P. (1990), Tidal dynamics of the water table in beaches, *Water Resour. Res.*, *26*(9), 2127–2134.

Nilson, R. H., and K. H. Lie (1990), Double-porosity modelling of oscillatory gas motion and contaminant transport in a fractured porous medium, *Int. J. Numer. Anal. Meteorol.*, *14*(8), 565–585.

Nilson, R. H., E. W. Peterson, K. H. Lie, N. R. Burkhard, and J. R. Hearst (1991), Atmospheric pumping: A mechanism causing vertical transport of contaminated gases through fractured permeable media, *J. Geophys. Res.*, *96*(B13), 21,933–21,948.

Noblanc, A., and H. J. Morel-Seytoux (1972), Perturbation analysis of two-phase infiltration, *J. Hydraul. Div.*, *98*(HY9), 1527–1541.

Norum, D. I., and J. N. Luthin (1968), The effects of entrapped air and barometric fluctuations on the drainage of porous mediums, *Water Resour. Res.*, *4*(2), 417–424.

O'Dwyer, T. P. (2010), The design of natural ventilation systems to control smoke movement in tunnels, *ASHRAE Trans.*, *116*(PT1), 3–10.

Olson, M. S., F. D. Tillman Jr., J. W. Choi, and J. A. Smith (2001), Comparison of three techniques to measure unsaturated-zone air permeability at Picatinny Arsenal, NJ, *J. Contam. Hydrol.*, *53*(1–2), 1–19.

Parker, J. C. (1989), Multiphase flow and transport in porous media, *Rev. Geophys.*, *27*(3), 311–328.

Parker, J. C. (2003), Physical processes affecting natural depletion of volatile chemicals in soil and groundwater, *Vadose Zone J.*, *2*(2), 222–230.

Parker, J. C., and R. J. Lenhard (1987), A model for hysteretic constitutive relations governing multiphase flow: 1. Saturation-pressure relations, *Water Resour. Res.*, *23*(12), 2187–2196.

Parker, J. C., R. J. Lenhard, and T. Kuppusamy (1987), A parametric model for constitutive properties governing multiphase flow in porous media, *Water Resour. Res.*, *23*(4), 618–624.

Parlange, J.-Y., and D. E. Hill (1979), Air and water movement in porous media: Compressibility effects, *Soil Sci.*, *127*(5), 257–263.

Peck, A. J. (1965a), Moisture profile development and air compression during water uptake by bounded porous bodies: 2. Horizontal columns, *Soil Sci.*, *99*(5), 327–334.

Peck, A. J. (1965b), Moisture profile development and air compression during water uptake by bounded porous bodies: 3. Vertical columns, *Soil Sci.*, *100*(1), 44–51.

Perrier, F., and P. Richon (2010), Spatiotemporal variation of radon and carbon dioxide concentrations in an underground quarry: Coupled processes of natural ventilation, barometric pumping and internal mixing, *J. Environ. Radioact.*, *101*(4), 279–296.

Perrier, F., P. Richon, C. Crouzeix, P. Morat, J.-L. LeMouël (2004), Radon-222 signatures of natural ventilation regimes in an underground quarry, *J. Environ. Radioact.*, *71*(1), 17–32.

Perrier, F., P. Richon, U. Gautam, D. R. Tiwari, P. Shrestha, and S. N. Sapkota (2007), Seasonal variations of natural ventilation and radon-222 exhalation in a slightly rising dead-end tunnel, *J. Environ. Radioact.*, *97*(2–3), 220–235.

Philip, J. R. (1975), Stability analysis of infiltration, *Soil Sci. Soc. Am. Proc.*, *39*(6), 1042–1049.

Pierdinock, M. J., and R. P. Fedder (1997), Bioslurping in a tidally-controlled formation: A case study, in *In Situ and On-Site Bioremediation, Volume 1: Papers From the Fourth International In Situ and On-Site Bioremediation Symposium*, New Orleans, 28 April—1 May 1997, pp. 285, Battelle, Columbus, Ohio.

Pinault, J.-L., and J.-C. Baubron (1996), Signal processing of soil gas radon, atmospheric pressure, moisture, and soil temperature data: A new approach for radon concentration modeling, *J. Geophys. Res.*, *101*(B2), 3157–3171.

Pinault, J.-L., and J.-C. Baubron (1997), Signal processing of diurnal and semidiurnal variations in radon and atmospheric pressure: A new tool for accurate in situ measurement of soil gas velocity, pressure gradient, and tortuosity, *J. Geophys. Res.*, *102*(B8), 18,101–18,120.

Pirkle, R. J., D. E. Wyatt, V. Price, and B. B. Looney (1992), Barometric pumping: The connection between the vadose zone and the atmosphere, in *Proceedings of the Focus Conference on Eastern Regional Ground Water Issues*, Boston, 13–15 Oct. 1992, pp. 427–439, Natl. Ground Water Assoc., Westerville, Ohio.

Pohl-Rüling, J., and E. Pohl (1969), The radon-222 concentration in the atmospheres of mines as a function of the barometric pressure, *Health Phys.*, *16*(5), 579–584.

Poulsen, T. G., and P. Møldrup (2006), Evaluating effects of wind-induced pressure fluctuations on soil-atmosphere gas exchange at a landfill using stochastic modelling, *Waste Manage. Res.*, *24*(5), 473–481.

Poulsen, T. G., and P. Sharma (2011), Apparent porous media gas dispersion in response to rapid pressure fluctuations, *Soil Sci.*, *176*(12), 635–641.

Poulsen, T. G., M. Christophersen, P. Moldrup, and P. Kjeldsen (2001), Modeling lateral gas transport in soil adjacent to old landfill, *J. Environ. Eng.*, *127*(2), 145–153.

Powers, W. L. (1934), Soil-water movement as affected by confined air, *J. Agric. Res.*, *49*(12), 1125–1133.

Pruess, K., C. Oldenburg, and G. Moridis (1999), TOUGH2 User's Guide, Version 2.0, *Rep. LBNL-43134*, Lawrence Berkeley Natl. Lab., Berkeley, Calif.

Prunty, L., and J. Bell (2007), Infiltration rate vs. gas composition and pressure in soil columns, *Soil Sci. Soc. Am. J.*, *71*(5), 1473–1475.

Prunty, L., and J. Bell (2008), Influence of pore gas on ponded infiltration into soil columns, in *Characterization, Monitoring, and Modeling of Geosystems: Proceedings of Sessions of Geocongress 2008,* New Orleans, Louisiana, 9–13 Mar 2008, edited by A. N. Alshawabkeh, K. R. Reddy, and M. V. Khire, pp. 84–91, Am. Soc. of Civ. Eng., Reston, Va.

Purtymun, W. D., F. C. Koopman, S. Barr, and W. E. Clements (1974), Air volume and energy transfer through test holes and atmospheric pressure effects on the main aquifer, *Los Alamos Sci. Lab. Informal Rep. LA-5725-MS*, Los Alamos, N. M.

Raats, P. A. C. (1973), Unstable wetting fronts in uniform and nonuniform soils, *Soil Sci. Soc. Am. Proc.*, *37*(5), 681–685.

Reddy, M. P. M. (2001), *Descriptive Physical Oceanography*, A. A. Balkema, Lisse, Netherlands.

Richards, L. A. (1931), Capillary conduction of liquids through porous mediums, *Physics*, *1*, 318–333.

Richon, P., F. Perrier, E. Pili, and J.-C. Sabroux (2009), Detectability and significance of 12 hr barometric tide in radon-222 signal, dripwater flow rate, air temperature and carbon dioxide concentration in an underground tunnel, *Geophys. J. Int.*, *176*(3), 683–694.

Richon, P., F. Perrier, J.-C. Sabroux, M. Trique, C. Ferry, V. Voisin, and E. Pili (2004), Spatial and time variations of radon-222 concentration in the atmosphere of a dead-end horizontal tunnel, *J. Environ. Radioact.*, *78*(2), 179–198.

Riha, B. D. (2005), Passive soil vapor extraction (PSVE) for VOC remediation at the Metallurgical Laboratory (MetLab) June 2005 progress report, *Rep. WSRC-TR-2005-00268*, U. S. Dep. of Energy, Washington, D. C.

Rogie, J. D., D. M. Kerrick, M. L. Sorey, G. Chiodini, and D. L. Galloway (2001), Dynamics of carbon dioxide emission at Mammoth Mountain, California, *Earth Planet. Sci. Lett.*, *188*(3–4), 535–541.

Rohay, V. J. (1996), Field tests of passive soil vapor extraction systems at the Hanford site, Washington, BHI-00766, Rev. 0, Bechtel Hanford, Richland, Wash.

Rohay, V. J., J. Rossabi, B. Looney, R. Cameron, and B. Peters (1993), Well venting and application of passive soil vapor extraction at Hanford and Savannah River, WHC-SA-2064-FP, ER 93-Environmental Remediation Conference, Augusta, Ga., 24–28 Oct.

Rojstaczer, S., and J. P. Tunks (1995), Field-based determination of air diffusivity using soil air and atmospheric pressure time series, *Water Resour. Res.*, *31*(12), 3337–3343.

Rossabi, J., and R. W. Falta (2002), Analytical solution for subsurface gas flow to a well induced by surface pressure fluctuations, *Ground Water*, *40(1)*, 67–75.

Rossabi, J., and B. D. Riha (1994), Passive control of VOCs using valved well heads: FY 1994 report (U), *Rep. WSRC-TR-94–0524*, Westinghouse Savannah River, Aiken, S C.

Rossabi, J., B. B. Looney, C. A. Eddy Dilck, B. Riha, and V. J. Rohay (1993), Passive remediation of chlorinated volatile organic compounds using barometric pumping, *Rep. WSRC-MS-93–615*, U.S. Dep. of Energy, Washington, D. C.

Rossabi, J., B. D. Riha, R. S. Vanpelt, T. Kmetz, and B. E. Pemberton (1998), Passive soil vapor extraction for interim remediation at the Savannah River site, in *Physical, Chemical, and Thermal Technologies: Remediation of Chlorinated and Recalcitrant Compounds: The First International Conference on Remediation of Chlorinated and Recalcitrant Compounds, Monterey, California*, 18–21 May 1998, edited by G. B. Wickramanayake and R. E. Hinchee, pp. 161–167, Battelle, Columbus, Ohio.

Sabeh, D. (2004), Adapting the Green and Ampt model to account for air compression and counterflow, MS thesis, Univ. South Florida, Tampa, Fla.

Sachs, T., C. Wille, J. Boike, and L. Kutzbach (2008), Environmental controls on ecosystem-scale CH_4 emission from polygonal tundra in the Lena River Delta, Siberia, *J. Geophys. Res.*, *113*, G00A03, doi:10.1029/2007JG000505.

Saffman, P. G., and G. Taylor (1958), The penetration of a fluid into a porous medium or Hele-Shaw cell containing a more viscous liquid, *Proc. R. Soc. London, Ser. A*, *245*(1242), 312–329.

Sambolek, M. (2004), Model testing of road tunnel ventilation in normal traffic conditions, *Eng. Struct.*, *26*(12), 1705–1711.

Sander, G., and J.-Y. Parlange (1984), Water and air movement in soils: An application of Brutsaert's and optimization techniques, *Soil Sci.*, *138*(3), 198–202.

Sander, G. C., J.-Y. Parlange, and W. L. Hogarth (1988), Air and water flow, II. Gravitational flow with an arbitrary flux boundary condition, *J. Hydrol.*, *99*(3–4), 225–234.

Sanford, R. L. (1982), Natural ventilation, in *Mine Ventilation and Air Conditioning*, 2nd ed., edited by H. L. Hartman, J. M. Mutmansky, and Y. J. Wang, pp. 239–253, John Wiley, New York.

Scanlon, B. R., and P. C. D. Milly (1994), Water and heat fluxes in desert soils 2. Numerical simulations, *Water Resour. Res.*, *30*(3), 721–733.

Scanlon, B. R., J. P. Nicot, and J. W. Massmann (2002), Soil gas movement in unsaturated systems, in *Soil Physics Companion*, edited by A. W. Warrick, CRC Press, Boca Raton, Fla.

Schery, S. D., and D. H. Gaeddert (1982), Measurements of the effect of cyclic atmospheric pressure variation on the flux of ^{222}Rn from the soil, *Geophys. Res. Lett.*, *9*(8), 835–838.

Schery, S. D., and A. G. Petschek (1983), Exhalation of radon and thoron: The question of the effect of thermal gradients in soil, *Earth Planet. Sci. Lett.*, *64*(1), 56–60.

Schery, S. D., and D. Siegel (1986), The role of channels in the transport of radon from the soil, *J. Geophys. Res.*, *91*(B12), 12,366–12,374.

Schery, S. D., D. H. Gaeddert, and M. H. Wilkening (1982), Transport of radon from fractured rock, *J. Geophys. Res.*, *87*(B4), 2969–2976.

Schery, S. D., D. H. Gaeddert, and M. H. Wilkening (1984), Factors affecting exhalation of radon from a gravelly sandy loam, *J. Geophys. Res.*, *89*(D5), 7299–7309.

Schery, S. D., S. Whittlestone, K. P. Hart, and S. E. Hill (1989), The flux of radon and thoron from Australian soils, *J. Geophys. Res.*, *94*(D6), 8567–8576.

Schubert, M., and H. Schulz (2002), Diurnal radon variations in the upper soil layers and at the soil-air interface related to meteorological parameters, *Health Phys.*, *83*(1), 91–96.

Schulz, W. H., J. W. Kean, and G. Wang (2009), Landslide movement in southwest Colorado triggered by atmospheric tides, *Nat. Geosci.*, *2*, 863–866.

Schumann, R. R., D. E. Owen, and S. Asher-Bolinder (1992), Effects of weather and soil characteristics on temporal variations in soil-gas radon concentrations, in *Geologic Controls on Radon*, edited by A. E. Gates and L. C. S. Gundersen, Geol. Soc. Am. Spec. Pap., 271, Boulder, Colo.

Schwander J., J.-M. Barnola, C. Andrié, M. Leuenberger, A. Ludin, D. Raynaud, and B. Stauffer (1993), The age of the air in the firn and the ice at Summit, *Greenland, J. Geophys. Res.*, *98*(D2), 2831–2838.

Scott, P. S., G. J. Farquhar, and N. Kouwen (1983), Hysteretic effects on net infiltration, in *Advances in Infiltration: Proceedings of the National Conference on Advances in Infiltration*, Hyatt Regency Illinois Center, Chicago, Illinois, 12–13 Dec. 1983, pp. 163–170, Am. Soc. of Agric. Eng., St. Joseph, Mich.

Scotter, D. R., and P. A. C. Raats (1969), Dispersion of water vapor in soil due to air turbulence, *Soil Sci.*, *108*(3), 170–176.

Segar, D. A. (1998), *Introduction to Ocean Sciences*, Wadsworth, Belmont, Calif.

Shan, C. (1995), Analytical solutions for determining vertical air permeability in unsaturated soils, *Water Resour. Res.*, *31*(9), 2193–2200.

Shan, C., I. Javandel, and P. A. Witherspoon (1999), Characterization of leaky faults: Study of air flow in faulted vadose zones, *Water Resour. Res.*, *35*(7), 2007–2013.

Shurpali, N. J., S. B. Verma, R. J. Clement, and D. P. Billesbach (1993), Seasonal distribution of methane flux in a Minnesota peatland measured by eddy correlation, *J. Geophys. Res.*, *98*(D11), 20,649–20,655.

Sillers, W. S., D. G. Fredlund, and N. Zakerzadeh (2001), Mathematical attributes of some soil-water characteristic curve models, *Geotech. Geol. Eng.*, *19*, 243–283.

Singh, M. M. (1982), Tunnel ventilation, in *Mine Ventilation and Air Conditioning*, 2nd ed., edited by H. L.Hartman, J. M. Mutmansky, and Y. J. Wang, pp. 453–481, John Wiley, New York.

Singh, V. P. (1997), *Kinematic Wave Modeling in Water Resources: Environmental Hydrology*, John Wiley, New York.

Slater, C. S., and H. G. Byers (1931), A laboratory study of the field percolation rates of soils, *U.S. Dep. of Agric. Tech. Bull. 232*, Washington, D. C.

Smetanová, I., K. Holý, M. Müllerová, and A. Polášková (2010), The effect of meteorological parameters on radon concentration in borehole air and water, *J. Radioanal. Nucl. Chem.*, *283*(1), 101–109.

Song, J.-Y., H. Li, and L. Wan (2013), Analytical study of airflow induced by barometric pressure and groundwater head fluctuations in a two-layered unsaturated zone, *Ground Water Monit. Rem.*, *33*(1), 40–47.

Sonu, J., and H. J. Morel-Seytoux (1976), Water and air movement in a bounded deep homogeneous soil, *J. Hydrol.*, *29*(1–2), 23–42.

Springer, D. S., S. J. Cullen, and L. G. Everett (1995), Laboratory studies on air permeability, in *Handbook of Vadose Zone Characterization and Monitoring*, edited by L. G. Wilson, L. G. Everett, and S. J. Cullen, pp. 217–247, Lewis Publishers, Boca Raton, Fla.

Stallman, R. W. (1967), Flow in the zone of aeration, in *Advances in Hydroscience*, vol. *4*, edited by V. T.Chow, pp. 151–195, Academic, New York.

Stallman, R. W., and E. P. Weeks (1969), The use of atmospherically induced gas-pressure fluctuations for computing hydraulic conductivity of the unsaturated zone (abs.), *Geol. Soc. Am. Abstr. Programs*, *7*, 213.

Starr, J. L., H. C. DeRoo, C. R. Frink, and J.-Y. Parlange (1978), Leaching characteristics of a layered field soil, *Soil Sci. Soc. Am. J.*, *42*(3), 386–391.

Steinitz, G., O. Piatibratova, and S. M. Barbosa (2007), Radon daily signals in the Elat Granite, southern Arava, Israel, *J. Geophys. Res.*, *112*, B10211, doi:10.1029/2006JB004817.

Stephens, D. B. (1996), *Vadose Zone Hydrology*, Lewis Publishers, Boca Raton, Fla.

Subke, J.-A., M. Reichstein, and J. D. Tenhunen (2003), Explaining temporal variation in soil CO_2 efflux in a mature spruce forest in Southern Germany, *Soil Biol. Biochem.*, *35*(11), 1467–1483.

Suhr, J. L., A. R. Jarrett, and J. R. Hoover (1984), The effect of soil air entrapment on erosion, *Trans. ASAE*, *27(1)*, 93–98.

Sun, H. (1997), A two-dimensional analytical solution of groundwater response to tidal loading in an estuary, *Water Resour. Res.*, *33*(6), 1429–1435.

Sundal, A. V., V. Valen, O. Soldal, and T. Strand (2008), The influence of meteorological parameters on soil radon levels in permeable glacial sediments, *Sci. Total Environ.*, *389*(2–3), 418–428.

Tanner, A. B. (1964), Radon migration in the ground: A review, in *The Natural Radiation Environment*, pp. 161–190, Univ. of Chicago Press, Chicago, Ill.

Thorstenson, D. C., and D. W. Pollock (1989a), Gas transport in unsaturated zones: Multicomponent systems and the adequacy of Fick's laws, *Water Resour. Res.*, *25*(3), 477–507.

Thorstenson, D. C., and D. W. Pollock (1989b), Gas transport in unsaturated porous media: The adequacy of Fick's law, *Rev. Geophys.*, *27*(1), 61–78.

Thorstenson, D. C., E. P. Weeks, H. Haas, E. Busenberg, L. N. Plummer, and C. A. Peters (1998), Chemistry of unsaturated zone gases sampled in open boreholes at the crest of Yucca Mountain, Nevada: Data and basic concepts of chemical and physical processes in the mountain, *Water Resour. Res.*, *34*(6), 1507–1529.

Tillman, F. D., Jr., and J. A. Smith (2005), Site characteristics controlling airflow in the shallow unsaturated zone in response to atmospheric pressure changes, *Environ. Eng. Sci.*, *22*(1), 25–37.

Thorstenson, D. C., E. P. Weeks, H. Haas, and J. C. Woodward (1989), Physical and chemical characteristics of topographically affected airflow in an open borehole at Yucca Mountain, Nevada, in *Focus 89 Proceedings on Nuclear Waste Isolation in the Unsaturated Zone*, Las Vegas, Nevada, 18–21 Sep. 1989, pp. 256–270.

Tillman, F. D., Jr., J.-W. Choi, W. Katchmark, J. A. Smith, and H. G. Wood III (2001), Unsaturated-zone airflow: Implications for natural remediation of groundwater by contaminant transport through the subsurface, in *Physicochemical Groundwater Remediation*, edited by J. A. Smith and S. E. Burns, pp. 307–339, Kluwer Acad., New York.

Todd, D. K. (1980), *Groundwater Hydrology*, 2nd ed., John Wiley, New York.

Tokida, T., T. Miyazaki, and M. Mizoguchi (2005), Ebullition of methane from peat with falling atmospheric pressure, *Geophys. Res. Lett.*, *32*, L13823, doi:10.1029/2005GL022949.

Tokida, T., T. Miyazaki, M. Mizoguchi, O. Nagata, F. Takakai, A. Kagemoto, and R. Hatano (2007), Falling atmospheric pressure as a trigger for methane ebullition from peatland, *Global Biogeochem. Cycles*, *21*, GB2003, doi:10.1029/2006GB002790.

Touma, J., and M. Vauclin (1986), Experimental and numerical analysis of two-phase infiltration in a partially saturated soil, *Transp. Porous Media*, *1(1)*, 27–55.

Touma, J., G. Vachaud, and J.-Y. Parlange (1984), Air and water flow in a sealed, ponded vertical soil column: Experiment and model, *Soil Sci.*, *137*(3), 181–187.

Tsang, Y. W., and K. Pruess (1989), Preliminary studies of gas phase flow effects and moisture migration at Yucca Mountain, Nevada, *Rep. LBL-28819*, Lawrence Berkeley Natl. Lab., Berkeley, Calif.

Tung, S., J. K. C. Leung, J. J. Jiao, J. Wiegand, and W. Wartenberg (2013), Assessment of soil radon potential in Hong Kong, China, using a 10-point evaluation system, *Environ. Earth Sci.*, *68*(3), 679–689.

Turcu, V. E., S. B. Jones, and D. Or (2005), Continuous soil carbon dioxide and oxygen measurements and estimation of gradient-based gaseous flux, *Vadose Zone J.*, *4*(4), 1161–1169.

Ursino, N., S. Silvestri, and M. Marani (2004), Subsurface flow and vegetation patterns in tidal environments, *Water Resour. Res.*, *40*, W05115, doi:10.1029/2003WR002702.

Vachaud, G., J. P. Gaudet, and V. Kuraz (1974), Air and water flow during ponded infiltration in a vertical bounded column of soil, *J. Hydrol.*, *22*(1–2), 89–108.

Vachaud, G., M. Vauclin, D. Khanji and M. Wakil (1973), Effects of air pressure on water flow in an unsaturated stratified vertical column of sand, *Water Resour. Res.*, *9*(1), 160–173.

van Genuchten, M. T. (1980), A closed-form equation for predicting the hydraulic conductivity of unsaturated soils, *Soil Sci. Soc. Am. J.*, *44*(5), 892–898.

van Genuchten, M. T., and D. R. Nielsen (1985), On describing and predicting the hydraulic properties of unsaturated soils, *Ann. Geophys.*, *3*(5), 615–628.

van Phuc, L., and H. J. Morel-Seytoux (1972), Effect of soil air movement and compressibility on infiltration rates, *Soil Sci. Soc. Am. Proc.*, *36*(2), 237–241.

Vauclin, M. (1989), Flow of water and air in soils: Theoretical and experimental aspects, in *Unsaturated Flow in Hydrologic Modeling, Theory and Practice*, edited by H. J. Morel-Seytoux, pp. 53–91, Kluwer Acad., Dordrecht, Netherlands.

Viveiros, F., T. Ferreira, J. Cabral Vieira, C. Silva, and J. L. Gaspar (2008), Environmental influences on soil CO_2 degassing at Furnas and Fogo volcanoes (São Miguel Island, Azores archipelago), *J. Volcanol. Geotherm. Res.*, *177*(4), 883–893.

Viveiros, F., T. Ferreira, C. Silva, and J. L. Gaspar (2009), Meteorological factors controlling soil gases and indoor CO_2 concentration: A permanent risk in degassing areas, *Sci. Total Environ.*, *407*(4), 1362–1372.

Waddington, E. D., J. Cunningham, and S. L. Harder (1996), The effects of snow ventilation on chemical concentrations, in *Chemical Exchange Between the Atmosphere and Polar Snow*, edited by E. W. Wolff, and R. C. Bales, pp. 403–451, NATO ASI Series, vol. *I* 43, Springer, Berlin.

Wala, A. M., J. R. Stoltz, E. Thompson, and S. Pattee (2002), Natural ventilation pressure in a deep salt mine—A case study, *Min. Eng.*, *54*(3), 37–42.

Wang, Z., J. Feyen, D. R. Nielsen, and M. T. vanGenuchten (1997), Two-phase flow infiltration equations accounting for air entrapment effects, *Water Resour. Res.*, *33*(12), 2759–2767.

Wang, Z., J. Feyen, M. T. vanGenuchten, and D. R. Nielsen (1998), Air entrapment effects on infiltration rate and flow instability, *Water Resour. Res.*, *34*(2), 213–222.

Wangemann, S. G., R. A. Kohl, and P. A. Molumeli (2000), Infiltration and percolation influenced by antecedent soil water content and air entrapment, *Trans. ASAE*, *43(6)*, 1517–1523.

Weeks, E. P. (1978), Field determination of vertical permeability to air in the unsaturated zone, *U.S. Geol. Surv. Prof. Pap.*, 1051.

Weeks, E. P. (1979), Barometric fluctuations in wells tapping deep unconfined aquifers, *Water Resour. Res.*, *15*(5), 1167–1176.

Weeks, E. P. (1987), Effect of topography on gas flow in unsaturated fractured rock: Concepts and observations, in *Flow and Transport Through Unsaturated Fractured Rock*, edited by D. D. Evans and T. J. Nicholson, pp. 165–170, AGU, Washington, D. C.

Weeks, E. P. (1991), Does the wind blow through Yucca Mountain? in *Proceedings of Workshop V: Flow and Transport Through Unsaturated Fractured Rock-Related to High-Level Radioactive Waste Disposal*, Radisson Suite Hotel, Tucson, Arizona, 7–10 Jan. 1991, edited by D. D. Evans and T. J. Nicholson, U.S. Nucl. Reg. Comm., NUREG/CP-0040, pp. 43–53.

Weeks, E. P. (2002), The Lisse effect revisited, *Ground Water*, *40(6)*, 652–656.

Weir, G. J., and W. M. Kissling (1992), The influence of airflow on the vertical infiltration of water into soil, *Water Resour. Res.*, *28*(10), 2765–2772.

Weisbrod, N., and M. I. Dragila (2006), Potential impact of convective fracture venting on salt-crust buildup and ground-water salinization in arid environments, *J. Arid. Environ.*, *65*(3), 386–399.

Weisbrod, N., M. I. Dragila, U. Nachshon, and M. Pillersdorf (2009), Falling through the cracks: The role of fractures in Earth-atmosphere gas exchange, *Geophys. Res. Lett.*, *36*, L02401, doi:10.1029/2008GL036096.

Whisler, F. D., and H. Bouwer (1970), Comparison of methods for calculating vertical drainage and infiltration for soils, *J. Hydrol.*, *10*(1), 1–19.

White, I., P. M. Colombera, and J. R. Philip (1977), Experimental studies of wetting front instability induced by gradual change of pressure gradient and by heterogeneous porous media, *Soil Sci. Soc. Am. J.*, *41*(3), 483–489.

Wigley, T. M. L. (1967), Non-steady flow through a porous medium and cave breathing, *J. Geophys. Res.*, *72*(12), 3199–3205.

Wilson, L. G., and J. N. Luthin (1963), Effect of air flow ahead of the wetting front on infiltration, *Soil Sci.*, *96*(2), 136–143.

Windsor, J., T. R. Moore, and N. T. Roulet (1992), Episodic fluxes of methane from subarctic fens, *Can. J. Soil Sci.*, *72*, 441–452.

Woodcock, A. H. (1987), Mountain breathing revisited-the hyperventilation of a volcano cinder cone, *Bull. Am. Meteorol. Soc.*, *68*(2), 125–130.

Woodcock, A. H., and I. Friedman (1979), Mountain breathing—Preliminary studies of air-land interaction on Mauna Kea, Hawaii, *U.S. Geol. Surv. Prof. Pap.*, 1123–A.

Wu, Y.-S., K. Pruess, and P. Persoff (1998), Gas flow in porous media with Klinkenberg effects, *Transp. Porous Media*, *32(1)*, 117–137.

Wu, Y.-S., K. Zhang, and H.-H. Liu (2006), Estimating large-scale fracture permeability of unsaturated rock using barometric pressure data, *Vadose Zone J.*, *5*(4), 1129–1142.

Xia, Y., H. Li, and L. Wang (2011), Tide-induced air pressure fluctuations in a coastal unsaturated zone: Effects of thin low-permeability pavements, *Ground Water Monit. Rem.*, *31*(2), 40–47.

You, K., H. Zhan, and J. Li (2010), A new solution and data analysis for gas flow to a barometric pumping well, *Adv. Water Resour.*, *33*(12), 1444–1455.

You, K., H. Zhan, and J. Li (2011), Gas flow to a barometric pumping well in a multilayer unsaturated zone, *Water Resour. Res.*, *47*, W05522, doi:10.1029/2010WR009411.

Young, A. (1990), Volumetric changes in landfill gas flux in response to variations in atmospheric pressure, *Waste Manage. Res.*, *8*(5), 379–385.

Young, A. (1992), The effects of fluctuations in atmospheric pressure on landfill gas migration and composition, *Water Air Soil Pollut.*, *64*(3–4), 601–616.

Youngs, E. G. (1995), Developments in the physics of infiltration, *Soil Sci. Soc. Am. J.*, *59*(2), 307–313.

Youngs, E. G., and A. J. Peck (1964), Moisture profile development and air compression during water uptake by bounded porous bodies: 1. Theoretical introduction, *Soil Sci.*, *98*(5), 290–294.

Zhang, Y., C. M. Oldenburg, and S. M. Benson (2004), Vadose zone remediation of carbon dioxide leakage from geologic carbon dioxide sequestration sites, *Vadose Zone J.*, *3*(3), 858–866.

Zimmerman, C., S. Larson, and R. Hoeppel (2003), Final report—Addendum—Natural pressure-driven passive bioventing, *Naval Facil. Eng. Serv. Cent. Tech. Rep.TR-2221-ENV*, Port Hueneme, Calif.

Zoran, M., R. Savastru, and D. Savastru (2012), Ground based radon (^{222}Rn) observations in Bucharest, Romania and their application to geophysics, *J. Radioanal. Nucl. Chem.*, *293*(3), 877–888.

Zyvoloski, G., Z. Dash, and S. Kelkar (1988), FEHM: Finite element heat and mass transfer code, *Rep. LA-11224-MS*, Los Alamos Natl. Lab., Los Alamos, N. M.